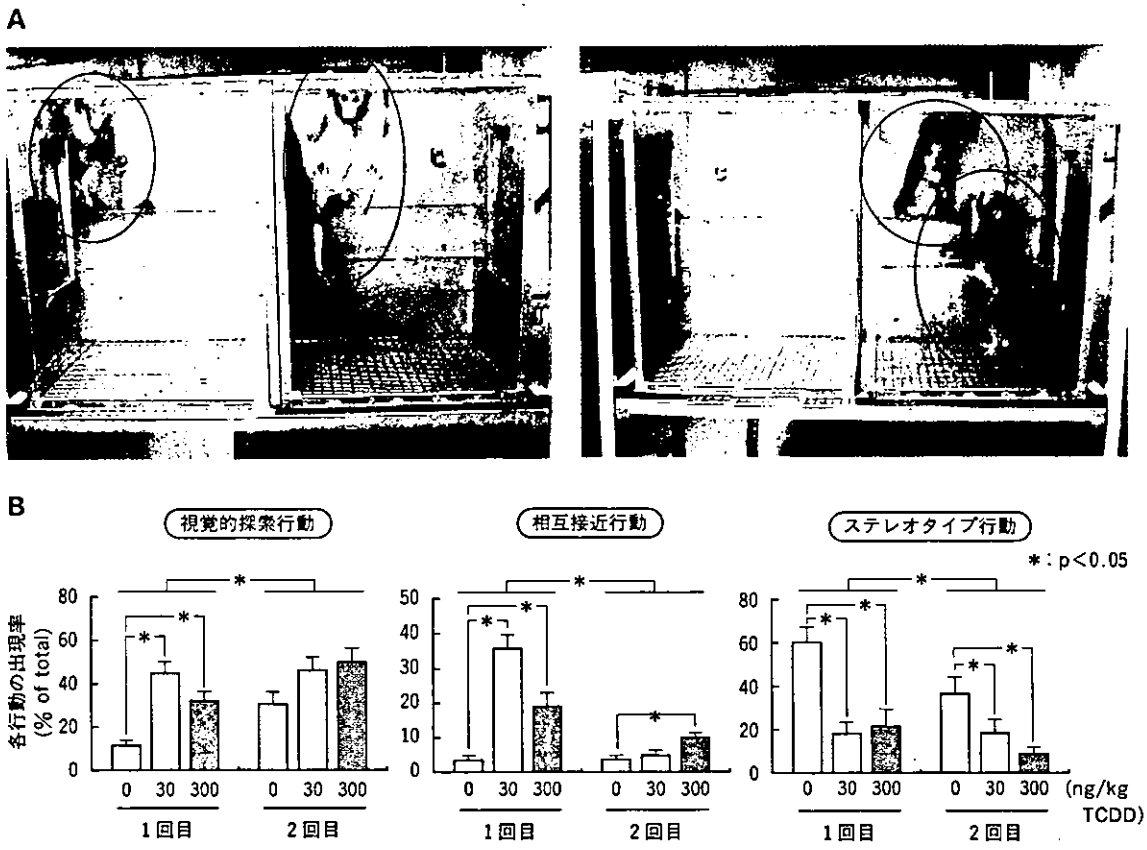

図1A　出会わせ試験用特別ケージ

2個の飼育ケージを連結し，中央を仕切りで区切り両側に被験個体を入れる(左)．仕切りを取り外すと2個体が接触し，さまざまな行動を示す(右)．

図1B　アカゲザルにおける胎生期・授乳期ダイオキシン曝露が社会性行動に与える影響

出会わせ試験は2回(1歳時，2歳時)を行った．ダイオキシン曝露(30，300 ng/kg 母体皮下投与)により視覚的探索行動の増加，相互接近行動の増加，ステレオタイプ行動の減少がみられた．1回目に比較し，2回目では影響が減少した．

グ法」を採用している[4]．もちろんこの試験は，解析段階においてビデオを観察する研究協力者のかなりの努力が必要であることを付け加えておく．

この試験を，実際に胎生期・授乳期にダイオキシン(2，3，7，8-TCDD)に曝露したアカゲザル個体について行った結果を紹介する(図1B)．ダイオキシンは妊娠20日目に30または300 ng/kgで母親に投与し，その後30日ごとに5％の追加投与を繰り返した．そこから生まれた次世代個体が1歳になった時1回目，2歳になった時に同様の組み合わせで2回目を行った．2回行ったのは，発達による変化も合わせて検討する目的があったためである．結果としてダイオキシン曝露個体同士の出会わせ試験では，対照群個体同士に比べ，出会わせテスト用特別ケージという新規場面における恐怖心が薄く，他個体に対してより多く接触を試みた．

また，この傾向は年齢を経るにつれ減少した．この結果は，数値としては明確であるが解釈は難しい．それでも，ダイオキシン曝露はアカゲザルにおいて，社会性に影響を与えると評価できる．さらに，世間を騒がせたダイオキシンは，少なくともサル類においては引きこもりなどの性格をもたらす原因ではないのかもしれない．

4段指迷路試験

この試験は，オリジナルに開発した記憶学習能力を測定する試験である[5]．指迷路は垂直方向に縦に並んだ4段の迷路(図2A)になっており，これを被験体が入れられた飼育ケージの扉に取り付けて用いる．迷路には各段1つの選択点が設けられており，このいずれかの選択点に置かれたリンゴ片を，サル類が装置のスリットから指を入れて正方向へ移動させればリンゴ片は下の段へと落ち，最終的にエサ箱からこのリンゴ片を取り出して食べることができる．一方，誤方向へ移動させるとリンゴ片は各段に設けられたエラーボックスへ落ち，サル類はこれを取り出すことができなくなる．このルールをいかに早く理解するかを指標とした学習能力試験である．

まず，装置に対する十分な馴化を行った後，指迷路の最下段である第1段の中央部に報酬となるリンゴ片を置き，これをエラーボックスに落とすことなくエサ箱まで指で運ぶ訓練を行う．15試行からなるセッションを1日2セッション行い，14試行以上が成功(エラーボックスに落とすことなくエサ箱に運ぶことのできる正反応)であるセッションが2セッション連続で起こることを学習基準とし，その次のセッションから順次課題を複雑化してゆく．つまり，次は2段目に報酬を置いて正しくエサ箱に運ぶことを学習させ(ただし，2段目の正方向は1段目と逆方向になっているので学習に時間を要する．以下3，4段目も正方向は下の段と逆方向となる)，次は3段目，4段目と進んでゆく．ある実験における集団がここまで学習するのに要した試行回数をグラフ化すると，図2Bのようになる．2段目を学習するのが特に難しいが，それを越えると楽になるというこ

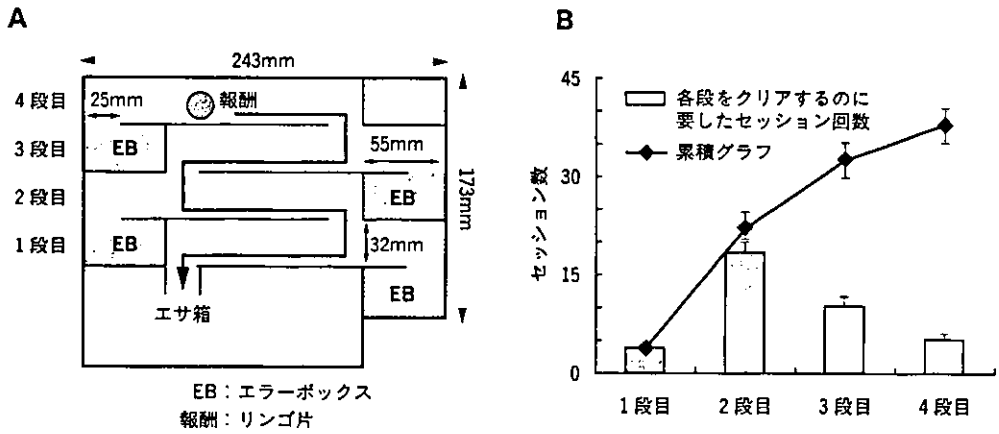

図2A　4段指迷路装置
サル類は報酬(リンゴ片)を得るために迷路のルールを学習する．

図2B　典型的な4段指迷路学習
1段目を学習した後，逆に動かさねばならない2段目の学習が特に時間がかかり，その後(3段目，4段目)はしだいにクリアするために要するセッション数が減少することがわかる．

とがグラフから読むことができる(図2B).

最後にランダム・テストというものを行う．ランダム・テストは迷路部1～4段のうちのいずれかに疑似ランダムな順番でリンゴ片を置き，エサ箱まで指で運べるか否かをテストする．これは，課題1～4において被験体が単に反応学習を行ったのではなく，指迷路の構造を理解し，課題解決の方法を習得しているか否かをテストするものである．

アイコンタクト試験

この試験もわれわれのオリジナルで，いまだ開発中である．前面が透明アクリル板になっている試験用ケージにサル類を入れ，その前に観察者が座り，被験サル類を見つめることで試験を開始する．サル類はもともとヒトと同様に，相手の目を見る性癖を持つことが知られており，1分間に目が合った回数をカウントするという至極単純な試験である．アイコンタクトを指標としている時点で，この試験はげっ歯類ではできない試験であるが，このアイコンタクトの回数がいったい何を意味しているかについても今後の検討課題である．それでもわれわれはこの試験から，被験サル類のヒト(飼育者，観察者)に対する反発的意識を測定できると考えている．もちろんこの試験は，新規場面における行動観察(ラットでいうオープンフィールドテスト)の亜型であるともいえる．通常の自発行動観察を目的とする試験では，この観察者というのは存在してはならず，ビデオカメラを用いてヒトを含む動くモノが被験サル類の視界に入らないようにするが，この試験はその逆を行っているのである．ことの発端は，多数のサル類に接するうちに，飼育者または観察者としてケージの前に立つと，こちらをにらみつける個体やこちらをちらりとも見ずにまるで目を合わせるのを避けるようにする個体がいて，しかもその性格(表現型)は個体内で固定しているような気がするという現場の意見であった．先の出会わせ試験では，同世代のサル類が相手で直接接触することが可能であるが，この試験では実験ケージの外にいる観察者に攻撃をしかけることはできない．また，相手もヒトであることから，この試験は単なるオープンフィールド，また出会わせ試験とも異なる形で被験サル類の外界に対する興味を数量化できる試験であると考えている．現在，開発中の試験であるため，この数値(アイコンタクトの回数)が脳機能の何に対応しているかといった情報は全くない．今後，向精神薬などを用い，薬理学的に脳内に負荷をかけた状態で本試験を行い「アイコンタクト」の脳内基盤を特定し，この回数の意味について理解を深めることに挑戦する予定である．この試験は，サル類を用いる行動試験の中でも最も簡便であることを特記しておく．また，観察者が男性であろうと女性であろうと，老若問わず，ある個体が示すアイコンタクトの回数はほぼ一定であることは確認済みである．また，発達につれてこの回数は増加する傾向にある．

薬物[illegible]試験

脳機能の発達障害といっても，正常状態では異常が顕在化せず，ある種のストレスなどにより極限状態になった時にのみ発現する行動異常もある．この試験の目的は，このような極限状態を薬理学的に作り出し評価し，さらにそこから神経伝達物質特異的な異常を探ることである．メタンフェタミンや，各種神経伝達物質特異的アゴニスト，アンタゴニストを投薬すると，サル類はその神経伝達物質依存の経路がかく乱され異常な行動(多動など)を示す．もしもある神経伝達物質の経路が障害されている場合，薬物に対する反応性が低下するはずであり，逆に亢進している場合は過敏になるはずである．この試験も現在，さまざまな条件検討を行っている最中である．

この方法論の利用例として，ラットにおいて周産期に内分泌かく乱化学物質としての疑いの強いビスフェノールAに曝露した次世代個体は，モノアミンオキシダーゼ阻害薬(トラニルサイプロミン)投与による活動量増加が起きなくなる，つまりこの薬物に対する反応性の消失がみられることが知られている[6]．未発表であるが，メタンフェタミンでも同様に反応性が低下していることを確認している．これらの事実から，たとえ無刺激の自発行動には異常がみられなくとも，脳内にはモ

ノアミン系の異常が潜んでおり，おそらくこの異常は，恐怖条件，極度のストレスを提示した際に露見する異常ともいえる．実際にこれらのラットは，電気刺激を用いた学習試験では異常をみせる．一方，従来の神経毒性試験などで用いられている自発運動量測定やオープンフィールド行動解析だけでは，この障害を検出することはできない．

話をサル類に戻すが，この試験はサル類で行う場合に特に重要な利点がある．それは，この試験はさまざまな薬物を投与することにより，貴重な次世代個体から次々と神経伝達物質別の異常の有無を評価できる可能性があるということである．この試験をさらに有用なものとするためには，特定の薬物で惹起される行動表現型をさまざまな薬物についてパターン化と定量化することが必須であり，現在，この作業を行って，近い将来実用に移したいと考えている．

おわりに

ここまでいろいろと毒性評価，特に脳機能の発達障害を評価するために有用と考えられるサル類を用いた行動試験法を紹介してきた．いまだ開発中のものが多いのは，サル類という動物が妊娠期間が160日程度，成熟するまでに数年かかることから，ラットのような時間軸では改良が進まないということでご理解いただきたい．それでもわれわれは，冒頭でも述べたように，サル類という実験動物を用いて発達障害の有無，程度を行動学的に評価することを優先してきた．当然のことながら次の疑問は，これらの試験法で検出できたサル類の行動発達障害はヒトに当てはめることができるのか？どう当てはめるのか？ということであろう．また，サル類におけるこの行動にはどういう意味があるのだろうという疑問も残る．今ここで，これらの疑問に明確に答えることは難しい．「発達障害の評価」の次には，最終的にはヒトに近縁である実験動物サル類における「発達障害の理解」を行動学的に行いたいが，そのためにはやはりここで紹介した試験系よりも，もっと高度で複雑な行動試験が要求されるであろう．それは今後に期待するしかない．また，サル類の行動に関する脳内基盤，特に分子生物学的情報とリンクさせる基礎実験が非常に重要であると考えられる．これについても現在，さまざまなアプローチを検討している．

ラットなどのげっ歯類に比べると，サル類は姿形だけでなく行動もヒトに似通っている．しかし，そのサル類でもヒトと全く同じとは言いがたい．そのうえ，ヒトと同様行動が複雑であるがゆえに，解釈に困る場合が多々ある．そこでわれわれは，最初から高度な機能障害の複雑さを理解するよりも先に，サル類において，より簡便に鋭敏に行動学的に発達障害を検出する系を目指しているのである．サル類の行動は，ヒトと同様に複雑であるがゆえに理解が難しいが，同じ理由で研究対象としてこれほど興味深く，かつヒトに外挿するのにこれほど有用なモデルも無いと考えている．

●文 献

1）Kimura N, Tanemura K, Nakamura S et al：Biochem Biophys Res Commun 310：303-311, 2003
2）Negishi T, Ishii Y, Kyuwa S et al：J Neurosci Methods 131：133-140, 2003
3）Schantz SL, Ferguson SA, Bowman RE：Neurotoxicol Teratol 14：433-446, 1992
4）Altmann J：Behaviour 49：227-267, 1974
5）Tsuchida J, Kawasaki K, Sankai T et al：Int J Primatol 24：261-270, 2003
6）Negishi T, Kawasaki K, Suzaki S et al：Environ Health Perspect 112：1159-1164, 2004

American Journal of Pathology, Vol. 165, No. 4, October 2004

Cell Injury, Repair, Aging and Apoptosis

Two Closely Related Ubiquitin C-Terminal Hydrolase Isozymes Function as Reciprocal Modulators of Germ Cell Apoptosis in Cryptorchid Testis

Jungkee Kwon,*† Yu-Lai Wang,* Rieko Setsuie,*‡ Satoshi Sekiguchi,† Yae Sato,*‡ Mikako Sakurai,*‡ Mami Noda,‡ Shunsuke Aoki,* Yasuhiro Yoshikawa,† and Keiji Wada*

From the Department of Degenerative Neurological Diseases, National Institute of Neuroscience, National Center of Neurology and Psychiatry, Kodaira, Tokyo; the Department of Biomedical Science,† Graduate School of Agricultural and Life Sciences, University of Tokyo, Tokyo; and the Laboratory of Pathophysiology,‡ Graduate School of Pharmaceutical Sciences, Kyushu University, Fukuoka, Japan*

The experimentally induced cryptorchid mouse model is useful for elucidating the *in vivo* molecular mechanism of germ cell apoptosis. Apoptosis, in general, is thought to be partly regulated by the ubiquitin-proteasome system. Here, we analyzed the function of two closely related members of the ubiquitin C-terminal hydrolase (UCH) family in testicular germ cell apoptosis experimentally induced by cryptorchidism. The two enzymes, UCH-L1 and UCH-L3, deubiquitinate ubiquitin-protein conjugates and control the cellular balance of ubiquitin. The testes of gracile axonal dystrophy (*gad*) mice, which lack UCH-L1, were resistant to cryptorchid stress-related injury and had reduced ubiquitin levels. The level of both anti-apoptotic (Bcl-2 family and XIAP) and prosurvival (pCREB and BDNF) proteins was significantly higher in *gad* mice after cryptorchid stress. In contrast, *Uchl3* knockout mice showed profound testicular atrophy and apoptotic germ cell loss after cryptorchid injury. Ubiquitin level was not significantly different between wild-type and *Uchl3* knockout mice, whereas the levels of Nedd8 and the apoptotic proteins p53, Bax, and caspase3 were elevated in *Uchl3* knockout mice. These results demonstrate that UCH-L1 and UCH-L3 function differentially to regulate the cellular levels of anti-apoptotic, prosurvival, and apoptotic proteins during testicular germ cell apoptosis. *(Am J Pathol 2004, 165:1367–1374)*

In the ubiquitin-proteasome system, the levels of poly- and monoubiquitin are strictly controlled by the balance of two groups of specific enzymes: ubiquitinating enzymes (E1, E2, and E3) and deubiquitinating enzymes (DUBs).[1,2] DUBs are subdivided into ubiquitin C-terminal hydrolases (UCHs) and ubiquitin-specific proteases (UBPs).[3,4] The genes for at least four UCHs, UCH-L1 and UCH-L3, UCH-L4, and UCH-L5, have been identified in mice.[5,6] Among them, UCH-L1 and UCH-L3 predominate; these isozymes have 52% amino acid identity and share significant structural similarity;[7] however, the distribution of these two isozymes is quite distinct in that UCH-L3 mRNA is expressed ubiquitously whereas UCH-L1 mRNA is selectively expressed in the testis/ovary and neuronal cells.[7–10] Despite the high-sequence homology, the *in vitro* hydrolytic activities of these two enzymes differ significantly. The activity (Kcat) of UCH-L3 is more than 200-fold higher than UCH-L1 when a fluorogenic ubiquitin substrate is used.[11] In addition to its relatively weak hydrolase activity, UCH-L1 exhibits dimerization-dependent ubiquityl ligase activity.[11] In contrast, UCH-L3 has little or no ligase activity compared with UCH-L1.[11] It was recently suggested that UCH-L1 has anti-proliferative activity in tumor cells, and that its expression is induced in response to tumor growth.[12] Furthermore, UCH-L1 associates with monoubiquitin and prolongs ubiquitin half-life in neurons.[13] Other work demonstrated that UCH-L3 binds to Nedd8 and subsequently processes its C-terminus.[14] Nedd8 is a small ubiquitin-like protein that shares with ubiquitin the ability to be conjugated to a lysine residue in a substrate protein.[15] Covalent conjugation of proteins by Nedd8 is an important form of the posttranscriptional modification and plays a critical role in many cellular processes.[16] These conju-

Supported by Grants-in-Aid for Scientific Research from the Ministry of Health, Labor, and Welfare of Japan; Grants-in-Aid for Scientific Research from the Ministry of Education, Culture, Sports, Science, and Technology of Japan; a grant from Pharmaceuticals and Medical Devices Agency of Japan; and a grant from Japan Science and Technology Agency.

Accepted for publication June 24, 2004.

Address reprint requests to Keiji Wada, Department of Degenerative Neurological Disease, National Institute of Neuroscience, National Center of Neurology and Psychiatry, Kodaira, Tokyo, 187-8502, Japan. E-mail: wada@ncnp.go.jp.

gates are regulated by a large number of deconjugating enzymes. This activity is unique to UCH-L3 because UCH-L1 is relatively weak to cleave the C terminus of Nedd8.[14–16] Collectively, these data suggest that the two mouse isozymes, UCH-L1 and UCH-L3, have distinct but overlapping functions. In addition, we recently found that *gad* mice, which lack UCH-L1 expression, show reduced retinal cell apoptosis in response to ischemia, suggesting that UCH-L1 may promote apoptosis.[17]

Our previous work focused on the possibility that UCH-L1 and UCH-L3 exhibit functional diversity during spermatogenesis. We showed that both UCH-L1 and UCH-L3 are strongly but reciprocally expressed in the testis during spermatogenesis,[18] suggesting that each isozyme may have a distinct function in the testis. To elucidate the pathophysiological roles of these two isozymes in the testis, our present work examines the extent of heat-induced stress using experimentally induced cryptorchidism in *Uchl3* knockout[7] and *gad* mice.[8] Normally, the testes are maintained in the scrotum at a temperature lower than that of the abdomen. Exposure of a testis to higher body temperature via experimentally induced cryptorchidism results in rapid degeneration of testicular germ cells.[19–22] Recent studies show that testicular germ cell degeneration in cryptorchid testes occurs via apoptosis, and that protein and lipid oxidation, along with p53 promote germ cell death.[23–25] The ubiquitin-proteasome system is required for the subsequent degradation of the damaged testicular germ cells.[26–28] Here, we show that both UCH-L1 and UCH-L3 have reciprocal functions in testicular germ cells during cryptorchid-induced apoptosis. Our data show that the absence of UCH-L1 causes resistance to cryptorchid-induced testicular germ cell apoptosis, and that the knockout of UCH-L3 promotes germ cell apoptosis after cryptorchid injury.

Materials and Methods

Animals

We used 8-week-old *Uchl3* knockout (C57BL/6J)[7,18] and *gad*[8,18,29] (CBA/RFM) male mice. *Uchl3* knockout mice were generated by the standard method using homologously recombinant ES cells, and the knockout line was back-crossed several times to C57BL/6J mice.[7] The *gad* mouse is an autosomal recessive mutant that was obtained by crossing CBA and RFM mice.[8] The *gad* line was maintained by intercrossing for more than 20 generations.[8,29] Both strains were maintained at our institute. Animal care and handling were in accordance with institutional regulations for animal care and were approved by the Animal Investigation Committee of the National Institute of Neuroscience, National Center of Neurology and Psychiatry, Tokyo, Japan.

Unilateral Experimental Cryptorchidism

Unilateral cryptorchidism was experimentally induced under pentobarbital anesthesia (Abbott Laboratories, North Chicago, IL).[20,22] Briefly, a midline abdominal incision was made, and the left testis was displaced from scrotum and fixed to the upper abdominal wall. The right testis remained in the scrotum as an intact control within the same animal. At 0, 4, 7, and 14 days after the operation, four control and four cryptorchid testes were harvested to determine testis weight.

Histological and Immunohistochemical Assessment of Testes

Testes were embedded in paraffin wax after fixation in 4% paraformaldehyde, sectioned at 4-μm thickness, and stained with hematoxylin and eosin.[29] Light microscopy was used for routine observations. For immunohistochemical staining, the sections were incubated with 10% goat serum for 1 hour at room temperature, followed by incubation overnight at 4°C with a rabbit polyclonal antibody against ubiquitin (1:500; DakoCytomation, Glostrup, Denmark) or Nedd8 (1:500; Alexis Biochemicals, San Diego, CA) diluted in phosphate-buffered saline (PBS) containing 1% bovine serum albumin. Sections were then incubated with fluorescein isothiocyanate-conjugated goat anti-rabbit IgG (1:200; Jackson ImmunoResearch, West Grove, PA) for 1 hour at room temperature and examined by confocal laser-scanning microscopy (Olympus, Tokyo, Japan).

Apoptotic cells in testicular tissues were identified by terminal deoxynucleotidyl transferase (TdT)-mediated nick-end labeling (TUNEL) using the DeadEnd Fluorimetric TUNEL system kit (Promega, Madison, WI) and the anti-PARP p85 fragment pAb (Promega) according to the manufacturer's instructions.

Quantitative Analysis of Apoptotic Germ Cells

The number of apoptotic cells was determined by counting the positively stained nuclei in 30 circular seminiferous tubule cross-sections per testis section.[23,29] The proportion of seminiferous tubules containing apoptotic germ cells was calculated by dividing the number of seminiferous tubules containing apoptotic cells by the total number of seminiferous tubules. The incidence of apoptotic cells per apoptotic cell-containing seminiferous tubule was categorized into three groups, defined as 1 to 5, 6 to 10, and >11 positive cells.

Western Blotting

Western blots were performed as previously reported.[8,18,29] Total protein (5 μg/lane) was subjected to sodium dodecyl sulfate-polyacrylamide gel electrophoresis using 15% gels (Perfect NT Gel; DRC, Japan). Proteins were electrophoretically transferred to polyvinylidene difluoride membranes (Bio-Rad, Hercules, CA) and blocked with 5% nonfat milk in TBS-T [50 mmol/L Tris base, pH 7.5, 150 mmol/L NaCl, 0.1% (w/v) Tween-20]. The membranes were incubated individually with one or more primary antibodies to UCH-L1 and UCH-L3 (1:1000; peptide antibodies[18]), Bcl-2, Bcl-xL, Bax, p53, and caspase-3, (1:1000; all from Cell Signaling Technology, Beverly, MA), phosphorylated cyclic AMP response element-binding protein (pCREB, 1:500; Upstate Biotech-

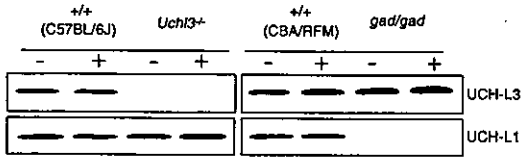

Figure 1. Western blotting analyses of both UCH-L3 and UCH-L1 in the testes of *gad* and *Uchl3* knockout mice, respectively, on day 4 after cryptorchid injury. Scrotal and cryptorchid testes did not differ significantly with respect to protein expression (−, scrotal testes; +, cryptorchid testes).

nology, Waltham, MA), brain-derived neurotrophic factor (BDNF, 1:500; Santa Cruz Biotechnology, Santa Cruz, CA), XIAP (1:500; Transduction Laboratories, Franklin Lakes, NJ), polyubiquitin (1:1000, clone FK-2; Medical & Biological Laboratories, Nagoya, Japan), monoubiquitin (1:1000, u5379; Sigma-Aldrich, St. Louis, MO), and Nedd8 (1:1000; Alexis Biochemicals, San Diego, CA). Blots were further incubated with peroxidase-conjugated goat anti-mouse IgG or goat anti-rabbit IgG (1:5000; Pierce, Rockford, IL) for 1 hour at room temperature. Immunoreactions were visualized using the SuperSignal West Dura extended duration substrate (Pierce) and analyzed with a Chemi-Imager (Alpha Innotech, San Leandro, CA). Each protein level was relatively quantificated after analysis with a ChemiImager using AlphaEase software.

Statistical Analysis

The mean and SD were calculated for all data (presented as mean ± SD). One-way analysis of variance was used for all statistical analyses.

Results

Level of Two UCH Isozymes in Scrotal and Cryptorchid Testes from Uchl3 Knockout and Gad Mice

We first confirmed the lack of UCH-L3 protein in the testes from *Uchl3* knockout mice by Western blotting (Figure 1). Similarly, we did not detect UCH-L1 protein in the testes of *gad* mice (Figure 1), as we previously observed.[13] Thus, in a biochemical sense, *gad* mice are analogous to *Uchl1*-null mice.[8,13] Compensatory level of UCH-L3 and UCH-L1 in *gad* and *Uchl3* knockout mice, respectively, was not observed (Figure 1; compare UCH-L3/UCH-L1 level with that of wild-type control mice). Experimental cryptorchidism did not affect UCH-L3 level in *gad* or wild-type control mice. Similarly, cryptorchidism did not affect UCH-L1 level in *Uchl3* knockout and wild-type control mice (Figure 1). Quantitative reverse transcriptase-polymerase chain reaction analysis showed that transcription from the *Uchl3* and *Uchl1* in both scrotal and cryptorchid testes from *gad* and *Uchl3* knockout mice was not significantly different from that measured in the corresponding wild-type control mice (data not shown). These results suggest that the level of UCH-L3 is regulated independently of UCH-L1 in the mouse testis, and that cryptorchid injury does not affect the level of either protein.

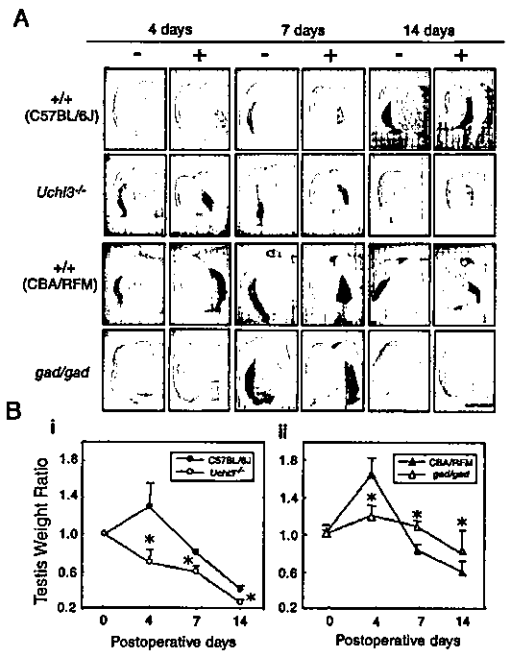

Figure 2. Comparison of testicular sizes and weights after experimental cryptorchidism. **A:** Gross images of changes in testicular size throughout time in two wild-type (C57BL/6J and CBA/RFM), *Uchl3* knockout, and *gad* mice (−, scrotal testes; +, cryptorchid testes). **B:** Ratio of cryptorchid to scrotal testis weight on days 0, 4, 7, and 14 after injury. **i:** Throughout time, the ratio for *Uchl3* knockout mice (**open circles**) differed significantly compared with wild-type mice (**filled circles**). ii: The ratio for *gad* mice (**open triangles**) did not differ significantly throughout time compared with wild-type mice (**closed triangles**). ($n = 4$; *, $P < 0.05$). Scale bar, 5 mm. Original magnifications, ×40.

Changes in Testicular Weight and Structure in Cryptorchid Uchl3 Knockout and Gad Mice

Unilateral cryptorchidism was surgically induced in *Uchl3* knockout and *gad* mice, and testes were evaluated on days 0, 4, 7, and 14 after the operation (Figure 2). Nonoperated (scrotal) testes served as controls for the evaluation of testicular weight and histochemistry. Cryptorchid testes from *Uchl3* knockout mice appeared smaller than the nonoperated controls at each time point, whereas the size of the cryptorchid testes from *gad* mice was similar to the controls (Figure 2A). Figure 2B shows the time course of the ratio of testicular weight of cryptorchid testes to scrotal testes. In wild-type mice (C57BL/6J and CBA/RFM), the ratio transiently increased 4 days after cryptorchid injury, most likely a consequence of inflammation-induced fluid accumulation[22,23] and biochemical changes observed. The ratio for these mice subsequently decreased below 1.0 by day 7. The ratio remained ~1.0 in *gad* mice (range,1.15 ~ 0.85), whereas it decreased significantly in *Uchl3* knockout mice compared with wild-type mice (Figure 2B). These results demonstrate that testes from *Uchl3* knockout and *gad* mice differ in their response to experimental cryptorchidism.

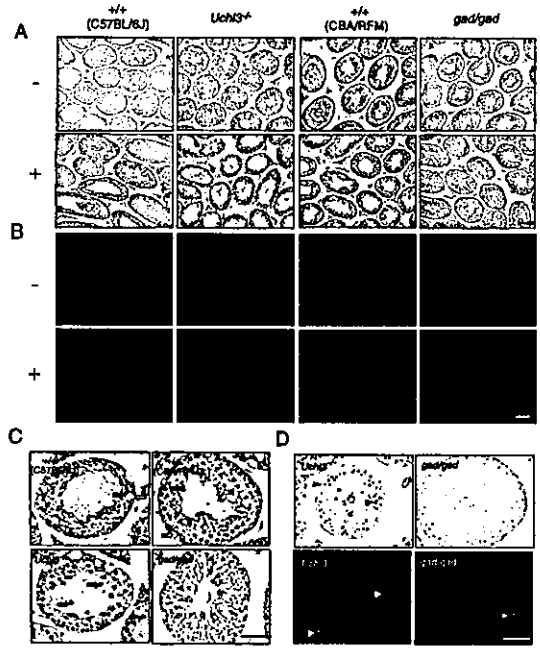

Figure 3. Histology and TUNEL staining of testicular cross sections after experimental cryptorchidism. **A:** Morphological analysis of seminiferous tubules on day 7 after cryptorchid injury. Note the germ cell loss and atrophy in cryptorchid testes compared with uninjured controls. (−, scrotal testes; +, cryptorchid testes). **B:** TUNEL staining of testicular cross-sections on day 7 after cryptorchid injury. Green fluorescence, TUNEL-positive cells; red fluorescence, nuclei stained with propidium iodide. **C:** Magnified cryptorchid testes sections. Pyknotic bodies (**filled arrows**) and Sertoli cell vacuolization (**open arrows**) were evident in cryptorchid testes of *Uchl3* knockout and the two wild-type (C57BL/6J and CBA/RFM) mice on day 7 after injury. **D:** PARP analysis to detect apoptotic germ cells in cryptorchid testes of *Uchl3* knockout and *gad* mice on day 7 after injury. The detection of apoptotic germ cells (**arrowheads, top**) by PARP analysis was consistent with that of apoptotic germ cells (**arrowheads, bottom**) by TUNEL analysis. Scale bar, 50 μm. Original magnifications: **A** and **B** ×100; **C** and **D** ×200.

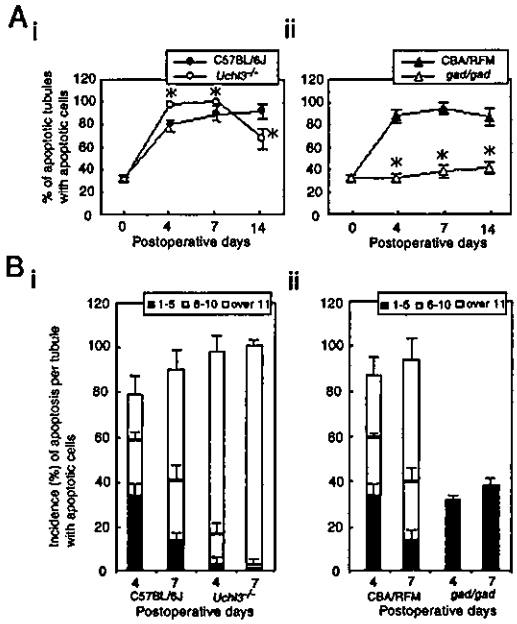

Figure 4. Quantitation of testicular germ cell apoptosis in testes after experimental cryptorchidism. **A:** The percentage of seminiferous tubules containing apoptotic germ cells in cryptorchid testes on days 0, 4, 7, and 14 after injury. **i:** The increase in the percentage of tubules containing apoptotic cells in the cryptorchid testes of *Uchl3* knockout mice is statistically significant compared with wild-type mice on days 4, 7, and 14. Each value represents the mean ± SD; *, $P < 0.05$. **ii:** The percentage of apoptotic tubules in cryptorchid testes of *gad* mice is significantly different on days 4, 7, and 14 after injury. Each value represents the mean ± SD; *, $P < 0.01$. **B:** Incidence of apoptosis per seminiferous tubule with apoptotic germ cells on days 4 and 7 after injury. The incidence of seminiferous tubules containing >11 apoptotic germ cells is significantly increased ($P < 0.05$) in cryptorchid testes of *Uchl3* knockout mice compared with wild-type mice. **i:** Comparison with *Uchl3* knockout mice. **ii:** Comparison with *gad* mice. Each value represents the mean ± SD.

Testicular Germ Cell Apoptosis in Cryptorchid Uchl3 Knockout and Gad Mice

To explore the mechanism underlying the observed differences between *Uchl3* knockout and *gad* cryptorchid testes, we prepared histological cross-sections on day 7 after testicular injury (Figure 3, A and C). The presence of nuclear pyknosis, multinucleated giant cells, and Sertoli cell vacuolization with germ cell loss in the germinal epithelium is indicative of cryptorchid testes.[22,23] These hallmarks of testicular injury were the most remarkable characteristics of cryptorchid testes from *Uchl3* knockout mice, demonstrating profound testicular atrophy and germ cell loss compared with wild-type mice (Figure 3, A and C). In contrast, no nuclear pyknosis, cellular shrinkage, or germ cell loss was observed in cryptorchid testes from *gad* mice. Spermatocytes and early spermatids comprised the majority of affected cell types in cryptorchid testes (Figure 3, A and C).

Germ cell apoptosis was further examined by TUNEL and PARP assays in tissue sections from postoperative day 7 mice (Figure 3, B and D). All but the *gad* cryptorchid testes showed a time-dependent increase in germ cell apoptosis during experimental cryptorchidism; germ cell apoptosis was always found in tubules that had germ cell loss on days 4, 7, and 14 (Figure 3, B and D, and Figure 4). Compared to wild-type mice, the cryptorchid testes of *Uchl3* knockout mice showed a marked increase in apoptotic germ cells in response to testicular injury, whereas *gad* mice lacked cryptorchid-induced germ cell apoptosis (Figure 3B and Figure 4). By postoperative days 4 and 7, the percentage of seminiferous tubules containing apoptotic germ cells increased with statistical significance ($n = 4$) ($P < 0.05$) in cryptorchid testes of *Uchl3* knockout mice as compared with wild-type mice (Figure 4A). In addition, cryptorchid testes of *Uchl3* knockout mice showed a high incidence of seminiferous tubules containing >11 apoptotic germ cells on days 4 and 7 days as compared with wild-type mice (Figure 4B); however, germ cell apoptosis did not increase in cryptorchid testes of *gad* mice during postoperative days 4 to 14 ($P < 0.01$) (Figure 4, A and B).

Cellular Mono- and Polyubiquitin Level in Cryptorchid Uchl3 Knockout and Gad Mice

Ubiquitin is required for energy-dependent degradation of structurally altered proteins.[26] We previously reported that UCH-L1 binds ubiquitin and stabilizes ubiquitin turnover in neurons, and that the level of monoubiquitin is decreased in *gad* mice.[13] In a model of ischemic insult in the retina, ubiquitin induction was unexpectedly lower and ischemic

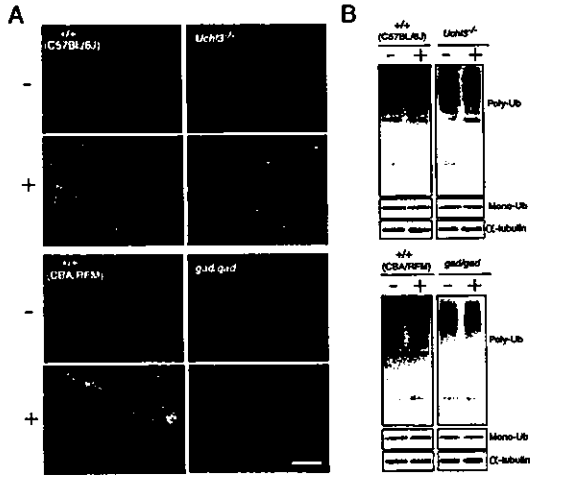

Figure 5. Immunohistochemical and Western blotting analyses of mono- and polyubiquitin in testes on day 7 after experimental cryptorchidism. **A:** Ubiquitin induction was not different between cryptorchid testes from *Uchl3* knockout and wild-type mice, whereas cryptorchid-induced ubiquitin induction in *gad* mice was reduced. Green fluorescence, ubiquitin-positive cells; red fluorescence, nuclei stained with propidium iodide. **B:** Polyubiquitin level in *Uchl3* knockout mice and the two wild-type (C57BL/6J and CBA/RFM) mice substantially increased after injury, whereas that in *gad* mice did not change significantly. Monoubiquitin level did not change after injury. Representative images from four independent experiments are shown (−, scrotal testes; +, cryptorchid testes). Scale bar, 50 μm. Original magnifications, ×200.

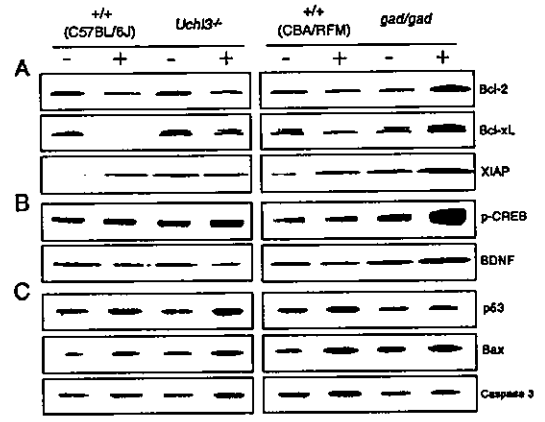

Figure 6. Western blotting analysis of anti-apoptotic, prosurvival, and apoptotic proteins in testes after experimental cryptorchidism. Total protein (5 μg per lane) was prepared from scrotal and cryptorchid testes on day 4 after cryptorchid injury. The expression levels of anti-apoptotic (**A**), prosurvival (**B**), and apoptotic (**C**) proteins in the cryptorchid testes of *Uchl3* knockout, *gad*, and the two wild-type (C57BL/6J and CBA/RFM) mice were significantly different compared with control mice. Representative images from four independent experiments are shown (−, scrotal testes; +, cryptorchid testes).

damage was weaker in the retina of *gad* mice (compared with wild-type mice) after ischemic insult.[17] To determine whether the increase in germ cell apoptosis in cryptorchid testes is associated with ubiquitin induction, we performed immunohistochemical analysis of testes from postoperative day 7 mice. Ubiquitin immunoreactivity increased substantially in cryptorchid testes from *Uchl3* knockout mice and the two wild-type mice, whereas those from *gad* mice showed only minor ubiquitin induction (Figure 5A). The scrotal testes of *Uchl3* knockout and *gad* mice did not show significant differences in ubiquitin induction compared with corresponding controls (Figure 5A). Interestingly, most of the increased ubiquitin induction was detected in spermatocytes and spermatids, consistent with the data on germ cell apoptosis after cryptorchid injury (Figure 3D and Figure 5A). Cryptorchid-induced polyubiquitin levels in the testes from *Uchl3* knockout and the two wild-type mice also increased substantially after injury, whereas the cryptorchid testes of *gad* mice showed no significant difference compared with scrotal testes (Figure 5B); however, the expression levels of monoubiquitin did not change significantly in any of the mice after cryptorchid injury.

Level of Anti-Apoptotic and Apoptotic Proteins in Cryptorchid Uchl3 Knockout and Gad Mice

We previously showed that anti-apoptotic proteins such as Bcl-2 and prosurvival proteins including phosphorylated cyclic AMP response element-binding protein (pCREB) are up-regulated in degenerated retina of *gad* mice.[17] These proteins are degraded by ubiquitination-mediated proteolysis.[30] We examined the expression of the Bcl-2 family proteins, XIAP, pCREB, and caspases to determine their role in testicular germ cell apoptosis after experimental cryptorchidism 4 days after injury in *Uchl3* knockout and *gad* mice. The level of anti-apoptotic proteins such as Bcl-2, Bcl-xL, and XIAP was up-regulated (323.8 ± 57.5, 262.3 ± 22.1, and 209.9 ± 11.7, respectively, as compared with wild type, 100) in the cryptorchid testes of *gad* mice compared with wild-type mice (Figure 6A). Additionally, pCREB, which is normally degraded in a ubiquitination-mediated manner,[30] was apparently highly up-regulated (259.0 ± 22.6, as compared with wild type, 100) in the cryptorchid testes of *gad* mice (Figure 6B). It has been demonstrated that pCREB activates genes that up-regulate trophic factors including BDNF.[31,32] Consistent with pCREB up-regulation, BDNF level also increased (203.0 ± 19.6, as compared with wild type, 100) in cryptorchid testes of *gad* mice (Figure 6B). Level was variable for anti-apoptotic, prosurvival, and apoptotic proteins in the cryptorchid testes of *Uchl3* knockout mice. The level of pCREB, p53, Bax, and caspase3 was slightly increased (169.9 ± 15.2, 152.6 ± 12.9, and 157.3 ± 14.0, respectively, as compared with scrotal testes, 100) in cryptorchid testes of *Uchl3* knockout mice compared with scrotal testes (Figure 6, B and C). Wild-type control mice had a similar expression level pattern except for pCREB. Because p53 acts as an upstream activator of Bax expression,[33] the observed Bax up-regulation after cryptorchid injury was consistent with the elevated p53 level in *Uchl3* knockout and wild-type control mice (Figure 6C). In contrast, BDNF was down-regulated (74.3 ± 7.7 as compared with wild type, 100) in cryptorchid testes of *Uchl3* knockout mice (Figure 6B). The down-regulation of BDNF combined with the up-regulation of pCREB suggests that BDNF might be regulated by another pathway that involves UCH-L3 but not pCREB.[34] Compared with scrotal testes, the expression of anti-apoptotic proteins decreased or was unchanged in cryptorchid testes of *Uchl3* knockout mice (Figure 6A).

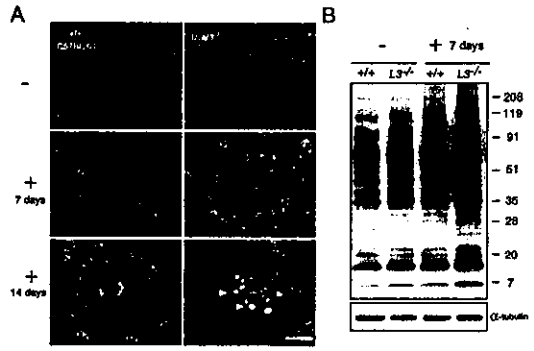

Figure 7. Immunohistochemical and Western blotting analyses of Nedd8 in testes from *Uchl3* knockout mice on days 7 and 14 after experimental cryptorchidism. **A:** Nedd8 induction in *Uchl3* knockout mice increased in both scrotal and cryptorchid testes. The shedding germ cells (**arrowheads**) in the cryptorchid testes of *Uchl3* knockout mice showed strong Nedd8 induction (−, scrotal testes; +7 days and + 4 days, cryptorchid testes). Green fluorescence, Nedd8-positive cells; red fluorescence, nuclei stained with propidium iodide. **B:** On day 7, the expression levels of Nedd8-conjugated proteins in *Uchl3* knockout mice were higher than in wild-type mice. Representative images of four independent experiments are shown. Scale bar, 50 μm. Original magnifications, ×200.

Nedd8 Level in Cryptorchid Uchl3 Knockout Mice

The varied expression levels of ubiquitin, anti-apoptotic, and apoptotic proteins in cryptorchid testes did not adequately explain the relatively exacerbated testicular atrophy and germ cell loss in *Uchl3* knockout mice compared with wild-type mice. We explored the underlying mechanism of this observation using the fact that UCH-L3 cleaves Nedd8.[14,16] We tested whether any change in Nedd8 expression correlated with greater testicular atrophy and germ cell loss in *Uchl3* knockout mice. Nedd8 immunoreactivity was highly detected in scrotal and cryptorchid testes from *Uchl3* knockout mice compared with wild-type mice (Figure 7A). The increased Nedd8 induction was mainly observed in spermatocytes and spermatids, and its expression pattern was similar to that of UCH-L3 during spermatogenesis.[18] These results suggest that Nedd8 may interact closely with UCH-L3 during testicular atrophy and germ cell loss. The cryptorchid testes of *Uchl3* knockout mice showed time-dependent and rapid Nedd8 induction compared with wild-type mice throughout the period 7 to 14 days after injury (Figure 7A). Moreover, the cryptorchid testes of *Uchl3* knockout mice showed strong Nedd8 induction in luminal shedding germ cells on day 14. An immunoblot of scrotal and cryptorchid testes proteins on day 7 confirmed the higher expression levels of Nedd8-conjugated proteins in *Uchl3* knockout mice as compared with wild-type mice (Figure 7B).

Discussion

During spermatogenesis, apoptosis controls germ cell numbers and eliminates defective germ cells to facilitate testicular homeostasis.[35–37] Recent studies indicate that ubiquitination targets proteins for degradation and modulates the turnover of various classes of short-lived signaling proteins.[28,38] Germ cell apoptosis after cryptorchid stress involves genes for various factors, such as Bcl-2 family proteins, p53, and caspases;[39–44] however, the impact of the ubiquitin system on the regulatory mechanisms of germ cell apoptosis is not fully understood. In a previous study, we used *gad* mice, which lack UCH-L1 expression, to show that neural cell apoptosis is suppressed after ischemic retinal injury *in vivo*.[17] These results suggest that UCH-L1 is involved in apoptosis-inducing pathways after stress. UCH-L1 and UCH-L3 are highly similar in sequence; however, UCH-L3 is expressed ubiquitously,[7] whereas UCH-L1 is selectively expressed in neurons and testes/ovaries.[8,9] We recently demonstrated that the expression of these UCH isozymes is differentially and developmentally regulated during spermatogenesis, and that UCH-L1 and UCH-L3 likely have distinct functions during different developmental phases.[18]

To understand the pathophysiological roles of UCH-L1 and UCH-L3 *in vivo*, two mutant mice, *Uchl3* knockout and *gad* mice, were examined after cryptorchid injury. The cryptorchid testes of the two mutant mice had fundamental differences after injury, in that testes of *Uchl3* knockout mice showed profound apoptosis-mediated germ cell loss, whereas *gad* mice were relatively resistant to injury (Figures 3 and 4). In addition, cryptorchid testes of *Uchl3* knockout mice showed greater testicular atrophy and germ cell loss than wild-type mice.

There are several proposed mechanisms for germ cell loss after experimental cryptorchidism.[21–23,45] The tumor suppressor protein, p53, is highly expressed in the testis and regulates both cell proliferation and apoptosis.[23,28,37] A role for p53 in experimental cryptorchidism has been demonstrated convincingly. The higher temperature of the testis caused by cryptorchidism induces p53-mediated apoptosis in the testis, and p53 overexpression results in increased germ cell apoptosis and decreased spermatozoa production.[23,46] In addition to p53, the Bcl-2 family and IAP (inhibitor of apoptosis protein) family are other major classes of intracellular apoptosis regulators.[47,48] The Bcl-2 family can be divided into anti-apoptotic members, such as Bcl-2, Bcl-xL, and Bcl-w, and proapoptotic members, such as Bax and Bak.[49] It has been suggested that the ratio of proapoptotic to anti-apoptotic Bcl-2 family members is important in determining whether a cell will undergo apoptosis.[49] A major function of the Bcl-2 family members appears to be the regulation of mitochondrial events, such as the release of proapoptotic factors.[50] The IAP family inhibits apoptosis primarily by inactivating and degrading proapoptotic proteins.[51] XIAP, a member of IAP family, can bind to and inhibit the proteinase activity of cellular caspase-3 and caspase-9, and thereby block the apoptotic process.[44,52,53]

With regard to cryptorchid injury, the balance between the expression of apoptosis-inducing and apoptosis-protecting proteins constitutes one possible mechanism underlying the observed germ cell apoptosis and protection from apoptosis in *Uchl3* knockout and *gad* mice, respectively. In *gad* mice, cryptorchid injury caused a large increase in the anti-apoptotic proteins Bcl-2, Bcl-xL, and XIAP, consistent with our previous report using retina.[17]

In addition, the expression levels of the prosurvival proteins pCREB and BDNF also increased in *gad* mice. Consistent with these results, caspase-3 expression was suppressed in *gad* mice. Cryptorchid testes of *Uchl3* knockout mice showed slightly increased expression of the apoptotic proteins p53, Bax, and caspase-3 after injury, although similar increases were also observed in wild-type control mice. In total, these results suggest that UCH-L1 plays a role in balancing the expression of apoptosis-inducing and apoptosis-protecting proteins. In contrast, UCH-L3 seems to resist germ cell apoptosis after cryptorchid injury.

Recent studies demonstrate that many molecules in the cellular apoptosis machinery, such as p53,[39,41] Bcl-2 family,[42,43,54] XIAP,[52] and caspase[44] members, are targets for ubiquitination.[28] This suggests that ubiquitination is one of the major mechanisms by which apoptotic cell death is regulated. UCH-L1 has been suggested to associate with monoubiquitin,[13] and the monoubiquitin pool is reduced in *gad* mice relative to wild-type mice. Protection from cryptorchid injury was reported in testes of mice expressing a mutant K48R ubiquitin,[22] suggesting that ubiquitin plays a critical role in processing or modulating testicular insults. Normally, damaged proteins are polyubiquitinated and degraded via the ubiquitin-proteasome system; however, if damaged proteins are not degraded as easily when monoubiquitin is either depleted or mutated, then germ cell death could be delayed.[17,22] Our results with the *gad* mouse suggest that ubiquitin induction plays a critical role in regulating cell death during cryptorchid injury-mediated germ cell apoptosis.

Uchl3 knockout mice exhibit severe retinal degeneration, suggesting that the UCH-L3-mediated ubiquitin pathway is involved in retinal homeostasis.[55] In the cryptorchid testes of *Uchl3* knockout mice, however, the profound testicular weight reduction and germ cell apoptosis after injury cannot be explained by ubiquitin induction alone. Our present results show that *Uchl3* knockout and wild-type mice have similar ubiquitin expression level in the testes, suggesting that UCH-L3 has another nonhydrolase activity in the ubiquitin-proteasome system. UCH-L3 also binds and cleaves the C-terminus of the ubiquitin-like protein, Nedd8.[14,56] This activity is unique to UCH-L3 because UCH-L1 does not cleave Nedd8. Thus, UCH-L3 appears to have dual affinities for ubiquitin and Nedd8. Our present results show that Nedd8 is strongly induced in scrotal testes of *Uchl3* knockout mice compared with those of wild-type mice (Figure 7). Cryptorchid testes of both *Uchl3* knockout and wild-type mice showed Nedd8 induction after injury, although the induction was higher in *Uchl3* knockout mice. These observations suggest that UCH-L3 may function as a deneddylating enzyme[16] *in vivo*, although further studies are necessary to clarify whether UCH-L3 interacts with Nedd8 during spermatogenesis.

In the present study, we demonstrate apparent reciprocal functions for the two deubiquitinating enzymes, UCH-L1 and UCH-L3, with respect to mediating injury after experimental cryptorchidism (Figure 8). Our results advance our understanding of the role of the ubiquitin-proteasome system in regulating apoptosis, and provide a unique opportunity for effective therapeutic intervention.

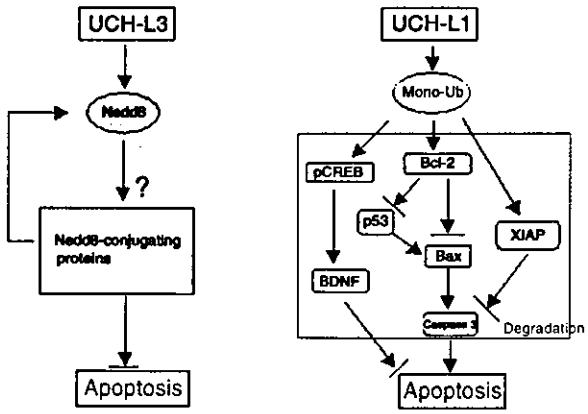

Figure 8. Differential function of the two UCH isozymes in response to experimental cryptorchidism. UCH-L3 has specificity for Nedd8. Cryptorchid injury results in protein damage and the accumulation of Nedd8-conjugated proteins. The accumulation of Nedd8-conjugated proteins in *Uchl3* knockout mice may contribute to profound germ cell loss via apoptosis. Hence, UCH-L3 might function as an anti-apoptotic regulator. UCH-L1 is involved in the maintenance of monoubiquitin levels. A deficiency in monoubiquitin results in delayed polyubiquitination and the accumulation of short-lived proteins after cryptorchid injury. Hence, UCH-L1 may function as a regulator of apoptosis.

Acknowledgments

We thank Dr. S.M. Tilghman for providing *Uchl3* knockout mice, H. Kikuchi for technical assistance with tissue sections, and M. Shikama for the care and breeding of animals.

References

1. Weissman AM: Themes and variations on ubiquitylation. Nat Rev Mol Cell Biol 2001, 2:169–178
2. Ciechanover A: The ubiquitin-proteasome pathway: on protein death and cell life. EMBO J 1998, 17:7151–7160
3. Pickart CM, Rose IA: Ubiquitin carboxyl-terminal hydrolase acts on ubiquitin carboxyl-terminal amides. J Biol Chem 1985, 260:7903–7910
4. Baker RT, Tobias JW, Varshavsky A: Ubiquitin-specific proteases of Saccharomyces cerevisiae. Cloning of UBP2 and UBP3, and functional analysis of the UBP gene family. J Biol Chem 1992, 267:23364–23375
5. Osawa Y, Wang YL, Osaka H, Aoki S, Wada K: Cloning, expression, and mapping of a mouse gene, Uchl4, highly homologous to human and mouse Uchl3. Biochem Biophys Res Commun 2001, 283:627–633
6. Kurihara LJ, Kikuchi T, Wada K, Tilghman SM: Loss of Uch-L1 and Uch-L3 leads to neurodegeneration, posterior paralysis and dysphagia. Hum Mol Genet 2001, 10:1963–1970
7. Kurihara LJ, Semenova E, Levorse JM, Tilghman SM: Expression and functional analysis of Uch-L3 during mouse development. Mol Cell Biol 2000, 20:2498–2504
8. Saigoh K, Wang YL, Suh JG, Yamanishi T, Sakai Y, Kiyosawa H, Harada T, Ichihara N, Wakana S, Kikuchi T, Wada K: Intragenic deletion in the gene encoding ubiquitin carboxy-terminal hydrolase in gad mice. Nat Genet 1999, 23:47–51
9. Kon Y, Endoh D, Iwanaga T: Expression of protein gene product 9.5, a neuronal ubiquitin C-terminal hydrolase, and its developing change in Sertoli cells of mouse testis. Mol Reprod Dev 1999, 54:333–341
10. Wilkinson KD, Deshpande S, Larsen CN: Comparisons of neuronal (PGP 9.5) and non-neuronal ubiquitin C-terminal hydrolases. Biochem Soc Trans 1992, 20:631–637
11. Liu Y, Fallon L, Lashuel HA, Liu Z, Lansbury Jr PT: The UCH-L1 gene

encodes two opposing enzymatic activities that affect alpha-synuclein degradation and Parkinson's disease susceptibility. Cell 2002, 111:209–218
12. Liu Y, Lashuel HA, Choi S, Xing X, Case A, Ni J, Yeh LA, Cuny GD, Stein RL, Lansbury Jr PT: Discovery of inhibitors that elucidate the role of UCH-L1 activity in the H1299 lung cancer cell line. Chem Biol 2003, 10:837–846
13. Osaka H, Wang YL, Takada K, Takizawa S, Setsuie R, Li H, Sato Y, Nishikawa K, Sun YJ, Sakurai M, Harada T, Hara Y, Kimura I, Chiba S, Namikawa K, Kiyama H, Noda M, Aoki S, Wada K: Ubiquitin carboxy-terminal hydrolase L1 binds to and stabilizes monoubiquitin in neuron. Hum Mol Genet 2003, 12:1945–1958
14. Wada H, Kito K, Caskey LS, Yeh ET, Kamitani T: Cleavage of the C-terminus of NEDD8 by UCH-L3. Biochem Biophys Res Commun 1998, 251:688–692
15. Hemelaar J, Borodovsky A, Kessler BM, Reverter D, Cook J, Kolli N, Gan-Erdene T, Wilkinson KD, Gill G, Lima CD, Ploegh HL, Ovaa H: Specific and covalent targeting of conjugating and deconjugating enzymes of ubiquitin-like proteins. Mol Cell Biol 2004, 24:84–95
16. Gong L, Kamitani T, Millas S, Yeh ET: Identification of a novel isopeptidase with dual specificity for ubiquitin- and NEDD8-conjugated proteins. J Biol Chem 2000, 275:14212–14216
17. Harada T, Harada C, Wang YL, Osaka H, Amanai K, Tanaka K, Takizawa S, Setsuie R, Sakurai M, Sato Y, Noda M, Wada K: Role of ubiquitin carboxy terminal hydrolase-L1 in neural cell apoptosis induced by ischemic retinal injury in vivo. Am J Pathol 2004, 164:59–64
18. Kwon J, Wang YL, Setsuie R, Sekiguchi S, Sakurai M, Sato Y, Lee WW, Ishii Y, Kyuwa S, Noda M, Wada K, Yoshikawa Y: Developmental regulation of ubiquitin C-terminal hydrolase isozyme expression during spermatogenesis in mice. Biol Reprod 2004, 71:515–521
19. Boekelheide K, Hall SJ: 2,5-Hexanedione exposure in the rat results in long-term testicular atrophy despite the presence of residual spermatogonia. J Androl 1991, 12:18–26
20. Ohta Y, Nishikawa A, Fukazawa Y, Urushitani H, Matsuzawa A, Nishina Y, Iguchi T: Apoptosis in adult mouse testis induced by experimental cryptorchidism. Acta Anat (Basel) 1996, 157:195–204
21. Yin Y, Hawkins KL, DeWolf WC, Morgentaler A: Heat stress causes testicular germ cell apoptosis in adult mice. J Androl 1997, 18:159–165
22. Rasoulpour RJ, Schoenfeld HA, Gray DA, Boekelheide K: Expression of a K48R mutant ubiquitin protects mouse testis from cryptorchid injury and aging. Am J Pathol 2003, 163:2595–2603
23. Yin Y, DeWolf WC, Morgentaler A: Experimental cryptorchidism induces testicular germ cell apoptosis by p53-dependent and -independent pathways in mice. Biol Reprod 1998, 58:492–496
24. Peltola V, Huhtaniemi I, Ahotupa M: Abdominal position of the rat testis is associated with high level of lipid peroxidation. Biol Reprod 1995, 53:1146–1150
25. Ahotupa M, Huhtaniemi I: Impaired detoxification of reactive oxygen and consequent oxidative stress in experimentally cryptorchid rat testis. Biol Reprod 1992, 46:1114–1118
26. Morimoto RI, Santoro MG: Stress-inducible responses and heat shock proteins: new pharmacologic targets for cytoprotection. Nature Biotechnol 1998, 16:833–838
27. Wojcik C: Proteasomes in apoptosis: villains or guardians? Cell Mol Life Sci 1999, 56:908–917
28. Yang Y, Yu X: Regulation of apoptosis: the ubiquitous way. EMBO J 2003, 17:790–799
29. Kwon J, Kikuchi T, Setsuie R, Ishii Y, Kyuwa S, Yoshikawa Y: Characterization of the testis in congenitally ubiquitin carboxy-terminal hydrolase-1 (Uch-L1) defective (gad) mice. Exp Anim 2003, 52:1–9
30. Taylor CT, Furuta GT, Synnestvedt K, Colgan SP: Phosphorylation-dependent targeting of cAMP response element binding protein to the ubiquitin/proteasome pathway in hypoxia. Proc Natl Acad Sci USA 2000, 97:12091–12096
31. Park C, Choi WS, Kwon H, Kwon YK: Temporal and spatial expression of neurotrophins and their receptors during male germ cell development. Mol Cells 2001, 12:360–367
32. Finkbeiner S: CREB couples neurotrophin signals to survival messages. Neuron 2000, 25:11–14
33. Selvakumaran M, Lin HK, Miyashita T, Wang HG, Krajewski S, Reed JC, Hoffman B, Liebermann D: Immediate early up-regulation of bax expression by p53 but not TGF beta 1: a paradigm for distinct apoptotic pathways. Oncogene 1994, 9:1791–1798
34. Liu L, Cavanaugh JE, Wang Y, Sakagami H, Mao Z, Xia Z: ERK5 activation of MEF2-mediated gene expression plays a critical role in BDNF-promoted survival of developing but not mature cortical neurons. Proc Natl Acad Sci USA 2003, 100:8532–8537
35. Matsui Y: Regulation of germ cell death in mammalian gonads. APMIS 1998, 106:142–148
36. Gosden R, Spears N: Programmed cell death in the reproductive system. Br Med Bull 1997, 53:644–661
37. Print CG, Loveland KL: Germ cell suicide: new insights into apoptosis during spermatogenesis. Bioessays 2000, 22:423–430
38. Lee JC, Peter ME: Regulation of apoptosis by ubiquitination. Immunol Rev 2003, 193:39–47
39. Haupt Y, Maya R, Kazaz A, Oren M: Mdm2 promotes the rapid degradation of p53. Nature 1997, 387:296–299
40. Oren M: Regulation of the p53 tumor suppressor protein. J Biol Chem 1999, 274:36031–36034
41. Ryan KM, Phillips AC, Vousden KH: Regulation and function of the p53 tumor suppressor protein. Curr Opin Cell Biol 2001, 13:332–337
42. Dimmeler S, Breitschopf K, Haendeler J, Zeiher AM: Dephosphorylation targets Bcl-2 for ubiquitin-dependent degradation: a link between the apoptosome and the proteasome pathway. J Exp Med 1999, 189:1815–1822
43. Marshansky V, Wang X, Bertrand R, Luo H, Duguid W, Chinnadurai G, Kanaan N, Vu MD, Wu J: Proteasomes modulate balance among proapoptotic and antiapoptotic Bcl-2 family members and compromise functioning of the electron transport chain in leukemic cells. J Immunol 2001, 166:3130–3142
44. Suzuki Y, Nakabayashi Y, Takahashi R: Ubiquitin-protein ligase activity of X-linked inhibitor of apoptosis protein promotes proteasomal degradation of caspase-3 and enhances its anti-apoptotic effect in Fas-induced cell death. Proc Natl Acad Sci USA 2001, 98:8662–8667
45. Yin Y, Stahl BC, DeWolf WC, Morgentaler A: P53 and Fas are sequential mechanisms of testicular germ cell apoptosis. J Androl 2002, 23:64–70
46. Ohta H, Aizawa S, Nishimune Y: Functional analysis of the p53 gene in apoptosis induced by heat stress or loss of stem cell factor signaling in mouse male germ cells. Biol Reprod 2003, 68:2249–2254
47. Beumer TL, Roepers-Gajadien HL, Gademan IS, Lock TM, Kal HB, De Rooij DG: Apoptosis regulation in the testis: involvement of Bcl-2 family members. Mol Reprod Dev 2000, 56:353–359
48. Oldereid NB, Angelis PD, Wiger R, Clausen OP: Expression of Bcl-2 family proteins and spontaneous apoptosis in normal human testis. Mol Hum Reprod 2001, 7:403–408
49. Borner C: The Bcl-2 protein family: sensors and checkpoints for life-or-death decisions. Mol Immunol 2003, 39:615–647
50. Yamamoto CM, Sinha Hikim AP, Huynh PN, Shapiro B, Lue Y, Salameh WA, Wang C, Swerdloff RS: Redistribution of Bax is an early step in an apoptotic pathway leading to germ cell death in rats, triggered by mild testicular hyperthermia. Biol Reprod 2000, 63: 1683–1690
51. Deveraux QL, Reed JC: IAP family proteins—suppressors of apoptosis. Genes Dev 1999, 13:239–252
52. Yang Y, Fang S, Jensen JP, Weissman AM, Ashwell JD: Ubiquitin protein ligase activity of IAPs and their degradation in proteasomes in response to apoptotic stimuli. Science 2000, 288:874–877
53. Deveraux QL, Roy N, Stennicke HR, Van Arsdale T, Zhou Q, Srinivasula SM, Alnemri ES, Salvesen GS, Reed JC: IAPs block apoptotic events induced by caspase-8 and cytochrome c by direct inhibition of distinct caspases. EMBO J 1998, 17:2215–2223
54. Li B, Dou QP: Bax degradation by the ubiquitin/proteasome-dependent pathway: involvement in tumor survival and progression. Proc Natl Acad Sci USA 2000, 97:3850–3855
55. Semenova E, Wang X, Jablonski MM, Levorse J, Tilghman SM: An engineered 800 kilobase deletion of Uchl3 and Lmo7 on mouse chromosome 14 causes defects in viability, postnatal growth and degeneration of muscle and retina. Hum Mol Genet 2003, 12:1301–1312
56. Dil Kuazi A, Kito K, Abe Y, Shin RW, Kamitani T, Ueda N: NEDD8 protein is involved in ubiquitinated inclusion bodies. J Pathol 2003, 199:259–266

Available online at www.sciencedirect.com

SCIENCE DIRECT

Brain Research 1019 (2004) 1–9

BRAIN RESEARCH

www.elsevier.com/locate/brainres

Research report

Accumulation of β- and γ-synucleins in the ubiquitin carboxyl-terminal hydrolase L1-deficient *gad* mouse

Yu-Lai Wang[a], Ayako Takeda[a], Hitoshi Osaka[a,b], Yoko Hara[a], Akiko Furuta[a], Rieko Setsuie[a,c], Ying-Jie Sun[a], Jungkee Kwon[a,d], Yae Sato[a,c], Mikako Sakurai[a,c], Mami Noda[c], Yasuhiro Yoshikawa[d], Keiji Wada[a,*]

[a] *Department of Degenerative Neurological Diseases, National Institute of Neuroscience, National Center of Neurology and Psychiatry, Kodaira, Tokyo 187-8502, Japan*

[b] *Information and Cellular Function, PRESTO, Japan Science and Technology Agency (JST), Kawaguchi, Saitama 332-0012, Japan*

[c] *Laboratory of Pathophysiology, Graduate School of Pharmaceutical Sciences, Kyushu University, Higashi, Fukuoka, 812-8582, Japan*

[d] *Department of Biomedical Science, Graduate School of Agricultural and Life Sciences, University of Tokyo, 1-1-1 Yayoi, Bunkyo, Tokyo, 113-8657, Japan*

Accepted 11 May 2004

Abstract

The synuclein family includes three isoforms, termed α, β and γ. α-Synuclein accumulates in various pathological lesions resulting from neurodegenerative disorders including Parkinson's disease (PD), dementia with Lewy bodies (DLB) and multiple system atrophy. However, neither β- nor γ-synuclein has been detected in Lewy bodies, and thus it is unclear whether these isoforms contribute to neurological pathology. In the present study, we used immunohistochemistry to demonstrate accelerated accumulation of β- and γ-synucleins in axonal spheroids in gracile axonal dystrophy (*gad*) mice, which do not express ubiquitin carboxyl-terminal hydrolase L1 (UCH-L1). γ-Synuclein immunoreactivity in the spheroids appeared in the gracile nucleus at 3 weeks of age and was maintained until 32 weeks. β-Synuclein immunoreactivity appeared in spheroids around 12 weeks of age. In contrast, α-synuclein immunoreactivity was barely detectable in spheroids. Immunoreactivity for synaptophysin and ubiquitin were either faint or undetectable in spheroids. Given that UCH-L1 deficiency results in axonal degeneration and spheroid formation, our findings suggest that β- and γ-synuclein participate in the pathogenesis of axonal swelling in *gad* mice.

Theme: Disorders of the nervous system
Topic: Degenerative disease: other

Keywords: Synuclein; Spheroid; UCH-L1; Ubiquitin

1. Introduction

The synucleins are a family of small cytosolic proteins that are expressed abundantly in the nervous system. Their contribution to neurophysiological function, however, is poorly understood. The mouse synuclein family consists of three members, α-synuclein (α-syn), β-synuclein (β-syn) and γ-synuclein (γ-syn), which range from 123 to 140 residues in length, exhibit 48–58% amino acid sequence identity and share similar domain organization (Fig. 1). Immunohistochemistry in the normal brain shows that α- and β-syn are concentrated at nerve terminals with little staining of somata and dendrites. Ultrastructural studies show that these isoforms localize to nerve terminals in close proximity to synaptic vesicles [18]. In contrast, γ-syn is present throughout nerve cells and is most abundant in the peripheral nervous system [5,18].

The synuclein family has been implicated in neurodegenerative diseases. Two point mutations (A53T, A30P) in the gene encoding α-synuclein (*SNCA*) have been detected in two distinct Parkinson's disease (PD) sibships with autosomal dominant inheritance [17,26], and a heritable

* Corresponding author. Tel.: +81-42-346-1715; fax: +81-42-346-1745.
E-mail address: wada@ncnp.go.jp (K. Wada).

0006-8993/$ - see front matter © 2004 Elsevier B.V. All rights reserved.
doi:10.1016/j.brainres.2004.05.023

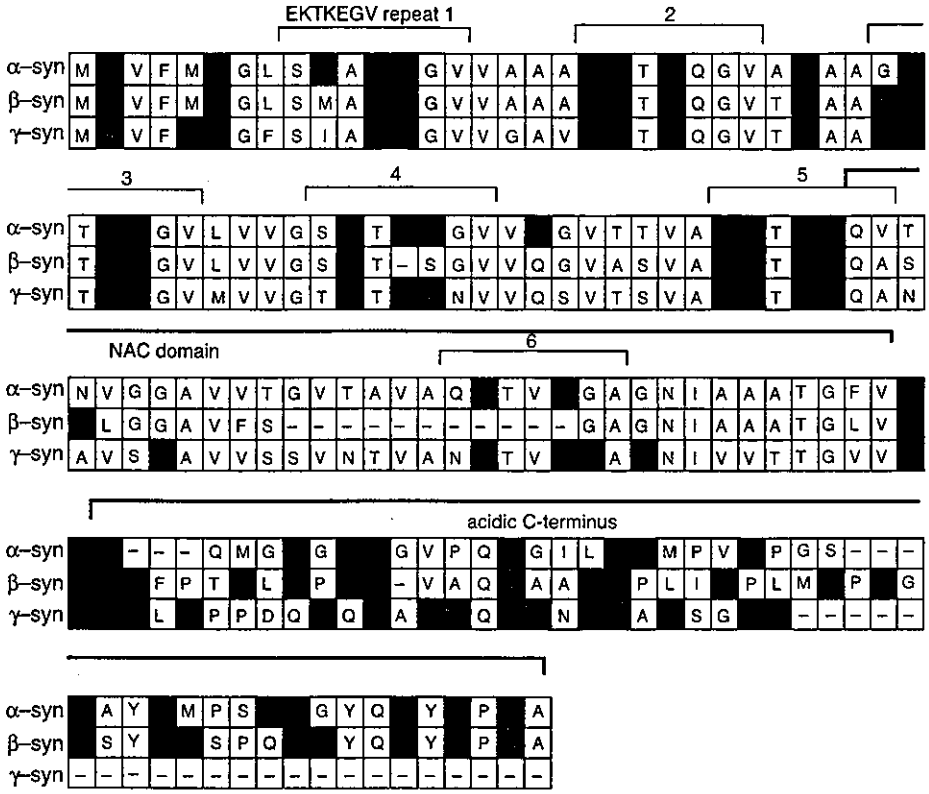

Fig. 1. Comparison of amino acid sequences from mouse α-, β- and γ-synuclein. The N-terminal region contains six imperfect repeats of the consensus EKTKEGV and the C-terminal region is negatively charged. A part of the hydrophobic NAC (non-amyloid component of amyloid plaque) domain is deleted in β-syn. Basic and acidic residues are shown in blue and red, respectively. Sequence accession numbers: mouse α-syn, NP-033247; mouse β-syn, NP-291088; mouse γ-syn, NP-035560.

genomic triplication of *SNCA* has been described within two distinct families [6,33]. Also, α-synuclein protein is a primary component of Lewy bodies (intracellular inclusions) and accumulates in abnormal neurites that contain ubiquitin, synaptophysin and neurofilaments [9,36,37]. β-Syn and γ-syn, which is also known as breast cancer-specific gene 1 (*BCSG1*), are overexpressed in neurodegenerative diseases such as PD and dementia with Lewy bodies (DLB) [5,7]. Unlike α- and β-syn, γ-syn is distributed throughout the cytoplasm of neurons where it influences the integration of neurofilament networks [4].

Ubiquitin carboxyl-terminal hydrolase L1 (UCH-L1) has been found throughout the brain and testis/ovary and has been considered as plays an important role in the labeling of abnormal proteins in the ubiquitin-proteasome system [15,38]. The gracile axonal dystrophy (*gad*) mouse is an autosomal recessive spontaneous mutant that was identified in 1984 [42]. It is the first mammalian neurological model with a defect in the ubiquitin-proteasome system [28]. These mice carry an intragenic deletion of the UCH-L1 gene (*Uchl1*) and do not express UCH-L1, making them comparable to a *Uchl1* null mutant [24,28]. The *gad* mouse exhibits severe sensory ataxia at an early stage, followed by motor paresis at a later stage [14,42]. In the central nervous system of *gad* mice, axonal degeneration begins from the distal ends of primary ascending axons in the dorsal root ganglia (DRG) [21,22]. Spheroid formation with the dying-back type of axonal degeneration is first observed in the gracile and dorsal spinocerebellar tracts [14,21,42]. In the most rostral portion of the gracile fascicles, spheroids are observed around 12 weeks of age and their formation progresses gradually to the terminal stage after 20 weeks of age [22]. At a later stage, axonal degeneration and spheroid formation are observed in the upper tracts of DRG neurons as well as in motor neurons [22]. Although the *gad* mutation is known to be caused by a deficiency in UCH-L1, the mechanism of spheroid formation is not well understood. Dystrophic axons or axonal spheroids have been observed in the brains of patients with infantile neuroaxonal dystrophy [1], in the globus pallidus in Hallervorden-Spatz disease [10], and in the gracile and cuneate nuclei in human vitamin-E deficiency [29]. Furthermore, spheroids are often observed in the medulla and spinal cords of aged mammals. In normal mice, the number of spheroids increases with age in the gracile nucleus [43].

Components of the spheroids of *gad* mice include amyloid-β protein, mitochondria, neurofilaments and synaptic complexes [12,22]. Ubiquitin and amyloid-β protein

also accumulate outside spheroids along the sensory and motor nervous systems [12,40]. We previously observed dot-like deposits of ubiquitin immunoreactivity throughout the gracile nucleus [40]. These data led us to suggest that the absence of functional UCH-L1 may affect the hydrolysis of unknown substrates, which could result in the formation of protein aggregates. α-Syn accumulation has been detected in spheroids resulting from type 1 iron accumulation in the brain (NBIA 1), a rare neurodegenerative disorder characterized by axonal spheroids and Lewy body-like intraneuronal inclusions [8]. Moreover, β-syn and γ-syn immunoreactivity were detected in spheroids but not in Lewy body-like inclusions [8]. In PD and DLB, axonal spheroid-like lesions were identified in the molecular layer of the dentate gyrus along with the accumulation of γ-syn, but not of α- or β-syn [7].

In the present study, we investigated the accumulation of α-syn, β-syn and γ-syn in the *gad* mouse using isoform-specific antibodies. Unexpectedly, we did not detect α-syn in spheroids, although β-syn and γ-syn accumulated in these structures beginning at an early stage of pathology. These results demonstrate that the *gad* mouse constitutes a useful model for investigating the role of synucleins in neurodegeneration.

2. Materials and methods

2.1. Animals

All mice were maintained and propagated at our institute. Adult homozygous *gad/gad* and wild-type (+/+) mice were obtained by mating heterozygous males with heterozygous females. All mouse experiments were performed in accordance with our institution's regulations for animal care and with the approval of the Animal Investigation Committee of the National Institute of Neuroscience, National Center of Neurology and Psychiatry. Each experimental group consisted of three male mice of the same phenotype, and experiments were conducted at 3 weeks (initial stage), 12 weeks (progressive stage), 17 and 20 weeks (critical stage), and 32 weeks (terminal stage) after birth [44].

2.2. Histochemistry

Mice were anesthetized and perfused with 0.9% NaCl followed by ice-cold 4% paraformaldehyde in phosphate-buffered saline (PBS, pH 7.4). Brains and spinal cords were then collected and postfixed in 4% paraformaldehyde overnight at 4 °C. The medulla oblongata and the upper cervical cord were examined. To ensure near complete concordance in the anatomical level of each sample, we followed the Atlas of the Mouse Brain and Spinal Cord [32]. Coronal sections were made at the level of the gracile nucleus (level 535) and of the cervical (C3) spinal cord segments. The samples were embedded in paraffin and sectioned (4 μm) for immunostaining and light microscopy. All sections from mice of the same age group were processed in parallel for each marker. Some sections were stained with hematoxylin–eosin (HE) and Klüver-Barrera for examination by conventional pathological methods. Quantification using stereological techniques was performed by counting eosinophilic spheroids at the medulla and upper cervical levels in at least three sections per sample by two blind observers. We then calculated the average number of spheroids per section. Spheroids were counted using the 200 × lens of a Zeiss Axioplan microscope. Under this magnification, eosinophilic spheroids are clearly viewed.

For immunohistochemistry, serial sections were deparaffinized in xylene and graded ethanol, washed in distilled water, and then treated with 0.3% H_2O_2 in methanol for 30 min to quench endogenous peroxidase activity. For the enhancement of α-syn immunostaining, sections were pretreated with 99% formic acid for 5 min or autoclaved at 121 °C for 10 min [35,36]. The sections were washed three times for 5 min in PBS, and then nonspecific binding sites were blocked by incubation in 10% normal serum obtained from the species in which the secondary antibody was generated. After a brief rinse with PBS, sections were incubated overnight at 4 °C with primary antibodies. Primary and secondary antibodies were diluted in DAKO Antibody Diluent (Dako, CA). The following antibodies were used at the final dilutions indicated: monoclonal α-syn antibody (1:100; BD Transduction Laboratories, CA), polyclonal β-syn antibody (1:200; Affinity Research Products), monoclonal synaptophysin antibody (1:50; Dako) and polyclonal ubiquitin antibody (1:400; Chemicon, Temecula). Polyclonal γ-syn antibody (see below) was diluted 1:100.

Subsequent antibody detection was carried out using anti-rabbit or anti-mouse IgG from the VECTASTAIN Elite ABC kit (Vector Labs, Burlingame, CA). Briefly, after washing, sections were sequentially incubated with biotinylated secondary antibodies for 1 h followed by avidin–biotin complex (diluted 1:200) for 1 h. Bound antibody complexes were visualized using 3,3′-diaminobenzidine tetrachloride as a peroxidase substrate. Sections were then lightly counterstained with hematoxylin. For the blocking experiments, anti-γ-syn was initially incubated with recombinant γ-syn for 4 h at 4 °C and the staining procedure was then performed as described above. The sections from different groups were immunostained and treated at the same time. For controls, the primary antibody was replaced with normal rabbit serum or was omitted (these controls always yielded negative staining).

2.3. Preparation of γ-syn antibody and antibody purification

γ-Syn cDNA was cloned from mouse brain mRNA using PCR with a primer set designed using the γ-syn nucleotide

sequence in GenBank (AF017255; sense primer, 5′-ACATGCATGCGACGTCTTCAAGAAAGGCTTC-3′; antisense primer, 5′-CCCAAGCTTGTCTTCTCCACTCTTGGC-3′). The γ-syn cDNA was cloned into the expression vector pEQ-30 (Qiagen, Germany), yielding a recombinant plasmid used to express histidine-tagged γ-syn (6-His-γ-syn) in *E. coli*. Recombinant 6-His-γ-syn was prepared as previously described [23] and used to generate a polyclonal antiserum in rabbits (Takara, Japan). The polyclonal antibodies were purified by affinity chromatography according to the manufacturer's instructions.

2.4. Specificities of synuclein antibodies

Purified recombinant α-syn (BD Transduction Laboratories), β-syn (Alpha Diagnostic International, TX) and γ-syn were diluted and subjected to electrophoresis through SDS-polyacrylamide gels (15% acrylamide) at 200, 100, 50, 25 and 12.5 ng per lane for each protein. The proteins were electrophoretically transferred to PVDF membranes (Bio-Rad, CA) as previously reported [23]. For immunochemical detection of the proteins, the membranes were first blocked in Tris-buffered saline containing 0.1% (w/v) Tween 20 (TTBS) and 3% BSA overnight at 4 °C and then incubated for 12 h with anti-α-syn (1:1000) or with anti-β- or anti-γ-syn (1:500). Antibodies were diluted in DAKO Antibody Diluent. The membranes were washed with TTBS and then incubated with horseradish peroxidase (HRP)-conjugated goat anti-rabbit or anti-mouse IgG (1:10,000; Pierce, IL) for 1 h. Proteins were detected using the SuperSignal chemiluminescence system (Pierce).

3. Results

3.1. Histopathological analysis of the gracile nucleus by HE staining

Oval or round spheroids were visualized by HE staining of axonal sections from wild-type mice at 20 weeks of age. However, fewer than five spheroids per section were detected. In contrast, gracile nuclei of *gad* mice exhibited both axonal dystrophy and spheroids as early as 3 weeks of age (Fig. 2A), in agreement with a previous report [44]. The number of spheroids increased with age, and the HE staining intensity of spheroids was relatively high until 20 weeks of age (Fig. 2B,C) but was very faint at 32 weeks (Fig. 2D). The size and appearance of the spheroids detected in *gad* mice varied with age. Irregularly shaped spheroids were observed from 12 to 20 weeks, whereas other spheroids stained diffusely or granularly as observed in wild-type mice (Fig. 2E). Some spheroids displayed an intense eosinophilic core, vacuoles or thin clefts (Fig. 2B).

We manually counted the total number of spheroids in the dorsal columns and dorsal nuclei of the medulla and upper cervical spinal cord using stereological techniques. Spheroids were detected in *gad* mice at all ages examined (Fig. 2F). The number of spheroids increased with age until 20 weeks (mean ± S.D.; $n = 8 \sim 13$): 3 weeks, 3.2 ± 0.8; 12 weeks, 12.1 ± 3.4; 20 weeks, 16.3 ± 3.9. At 32 weeks, however, the number of spheroids decreased (7.8 ± 2.2), as did their size (data not shown). These observations most likely reflect the severity of degeneration following the progression of the dying-back type of axonal dystrophy [14,44] to the lower spinal cord. In comparison, only a very

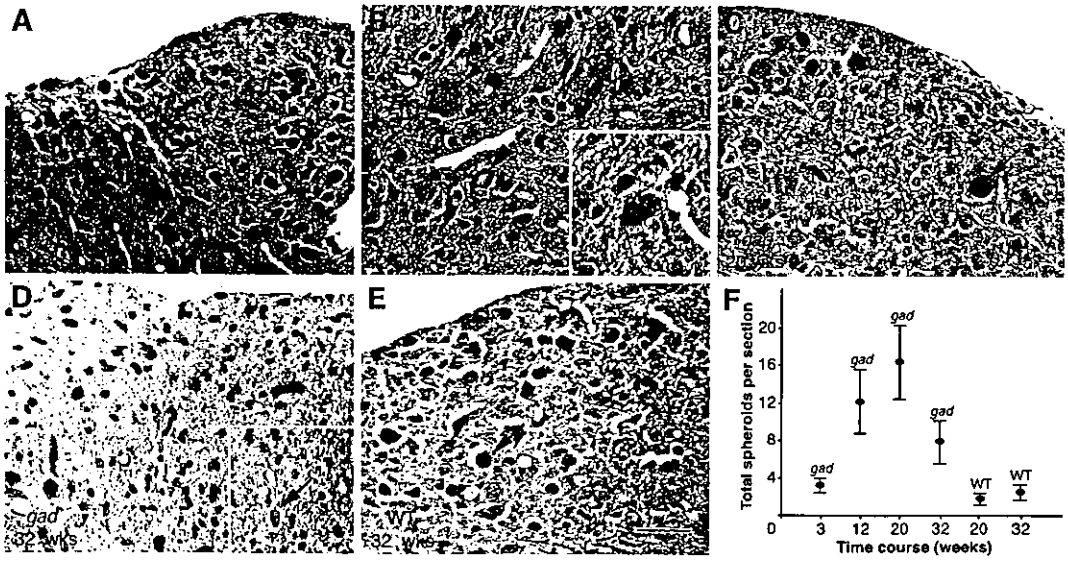

Fig. 2. Hematoxylin–eosin staining of eosinophilic spheroids (arrows) in (A–D) gad sections of the gracile nucleus of the medulla oblongata at 3, 12, 20 and 32 weeks of age, respectively, and in (E) a wild-type section at 32 weeks. An arrowhead indicates a vacuolar spheroid body, and a white arrow indicates a spheroid with an intense eosinophilic core (inset in B). (F) A quantitative study of spheroid number over time in gad and WT mice. Values are the mean ± S.D. ($n = 8 \sim 13$). Bar = 50 μm.

small number of spheroids were found in wild-type mice (1.8±0.6 at 20 weeks, 2.5 ± 0.8 at 32 weeks; $n = 9$; Fig. 2F).

3.2. Spheroids of gad mice accumulate β-syn and γ-syn but lack α-syn

We tested the specificity of the synuclein antibodies using purified recombinant synuclein isoforms. Polyclonal anti-γ-syn recognized purified recombinant γ-syn but did not cross-react with recombinant α-syn or β-syn in western blots (Fig. 3C). This antibody was also useful for immunohistochemical detection of γ-syn in spheroids in the gracile nucleus (Fig. 4A–D). No staining was observed when polyclonal anti-γ-syn was pre-absorbed with recombinant γ-syn (1:20 antibody/protein molar ratio; data not shown), thereby demonstrating the specificity of the staining. Under the same conditions, controls without anti-γ-syn showed no immunoreactivity (data not shown). An assay of specificity was also performed using the commercial antibodies against α-syn and β-syn, and similar results were obtained for both antibodies (Fig. 3A,B).

We then utilized all three isoform-specific antibodies to characterize the pathology of axonal degeneration in the *gad* mouse. Immunoreactivity to γ-syn was robust during postnatal weeks 3 ~ 20 but was weak at week 32 (Table 1). At 3 weeks of age, the spheroids detected by anti-γ-syn were more clearly recognized than those detected by HE staining. γ-Syn-immunoreactive spheroids varied in appearance as shown by HE staining (Fig. 2A–D), and oval or round spheroids were often diffusely or granularly immunostained

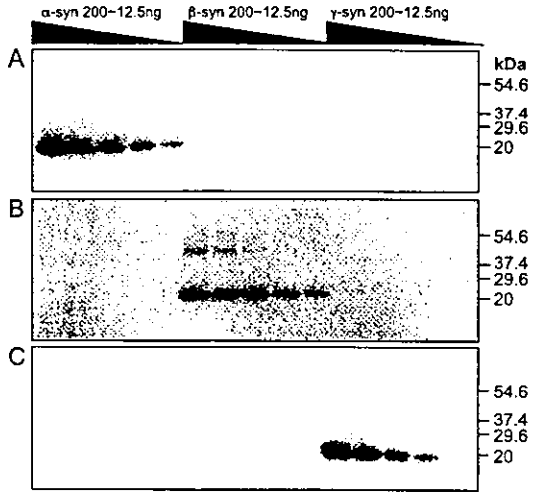

Fig. 3. Specificity of synuclein antibodies. Western blots show the specificity and reactivity of anti-α-syn, anti-β-syn and anti-γ-syn with varying amounts (12.5 ~ 200 ng) of all three recombinant synucleins. Three identical SDS-polyacrylamide gels were transferred to membranes under identical conditions, and each membrane was then probed separately with one of the synuclein antibodies. (A) α-syn antibody. (B) β-syn antibody. (C) γ-syn antibody. None of the antibodies exhibited significant cross-reactivity. A dimer formation (~ 50 kDa) was seen in the β-syn blot (B). Molecular weight markers (in kDa) are shown to the right.

by anti-γ-syn (Fig. 4A–C). Numerous dystrophic axons also displayed γ-syn immunoreactivity. γ-Syn immunoreactivity was absent both in spheroids and dystrophic axons when anti-γ-syn was pre-incubated with excess purified γ-syn (data not shown). In contrast to γ-syn immunoreactivity, spheroids started to exhibit faint and sporadic β-syn immunostaining from 12 weeks of age, with the intensity increasing through 32 weeks (Fig. 4E,F and Table 1). At 32 weeks, relatively intense β-syn staining was observed in spheroids and dystrophic axons (Fig. 4G); however, there were fewer immunopositive spheroids than were seen by γ-syn staining (at 20 weeks; Fig. 4C). Coarse granules around neurons were also immunostained by anti-β-syn (Fig. 4G). Very little α-syn immunoreactivity was observed in spheroids even after enhancement with formic acid or by autoclaving (Fig. 4I). These pretreatments also failed to show α-syn immunoreactivity in axons (Fig. 4I).

In wild-type mice, spheroids were immunopositive for γ-syn (Fig. 4D) and β-syn (a relatively weak punctate pattern in the center of spheroids; Fig. 4H). However, no α-syn immunoreactivity was detected (Fig. 4J, arrows). Also, ubiquitin-positive immunostaining, which did not appear until 20 weeks, was seen in spheroids and as dots that did not correspond to spheroids (data not shown). In *gad* mice, ubiquitin-immunoreactive dots appeared from 12 weeks of age as previously demonstrated [40] and spheroids were not immunoreactive for ubiquitin (Fig. 4K). Ubiquitin staining in general was more intense in the wild-type tissue (Fig. 4L) than in *gad* tissue (Fig. 4K). For synaptophysin, the limited number of spheroids were immunopositive in both wild-type and *gad* mice at 20 weeks of age, with a diffuse or spotty staining in the center of the spheroids (Fig. 4M,O). The *gad* mouse appears to show higher synaptophysin expression than wild-type mice (Fig. 4M,O). At 32 weeks, *gad* mice displayed a punctate distribution pattern of synaptophysin along synapses or surrounding cell bodies with a few densely stained spheroids (Fig. 4N, arrow). In contrast, wild-type mice displayed an expression pattern that was enriched in the spheroids at 32 weeks of age (Fig. 4P, arrow). Furthermore, *gad* mice exhibited dot-like immunostaining for ubiquitin (Fig. 4L, arrowheads), β-syn (Fig. 4G) and γ-syn (Fig. 4C).

4. Discussion

Previous studies of *gad* mice showed axonal degeneration and spheroid-formation (axonal dystrophy) in the gracile tract during the initial stage of neuropathology [14,22,44]. During the critical stage from 17 to 20 weeks of age, the pathological changes extend to the spinocerebellar tract and spinal trigeminal nucleus. During the terminal stage (beyond 32 weeks), these changes extend to the corticospinal tract, cuneate tract, spinal trigeminal tract and thalamus [44]. Although synucleins have been implicated in the pathology of various neurodegenerative disorders, the

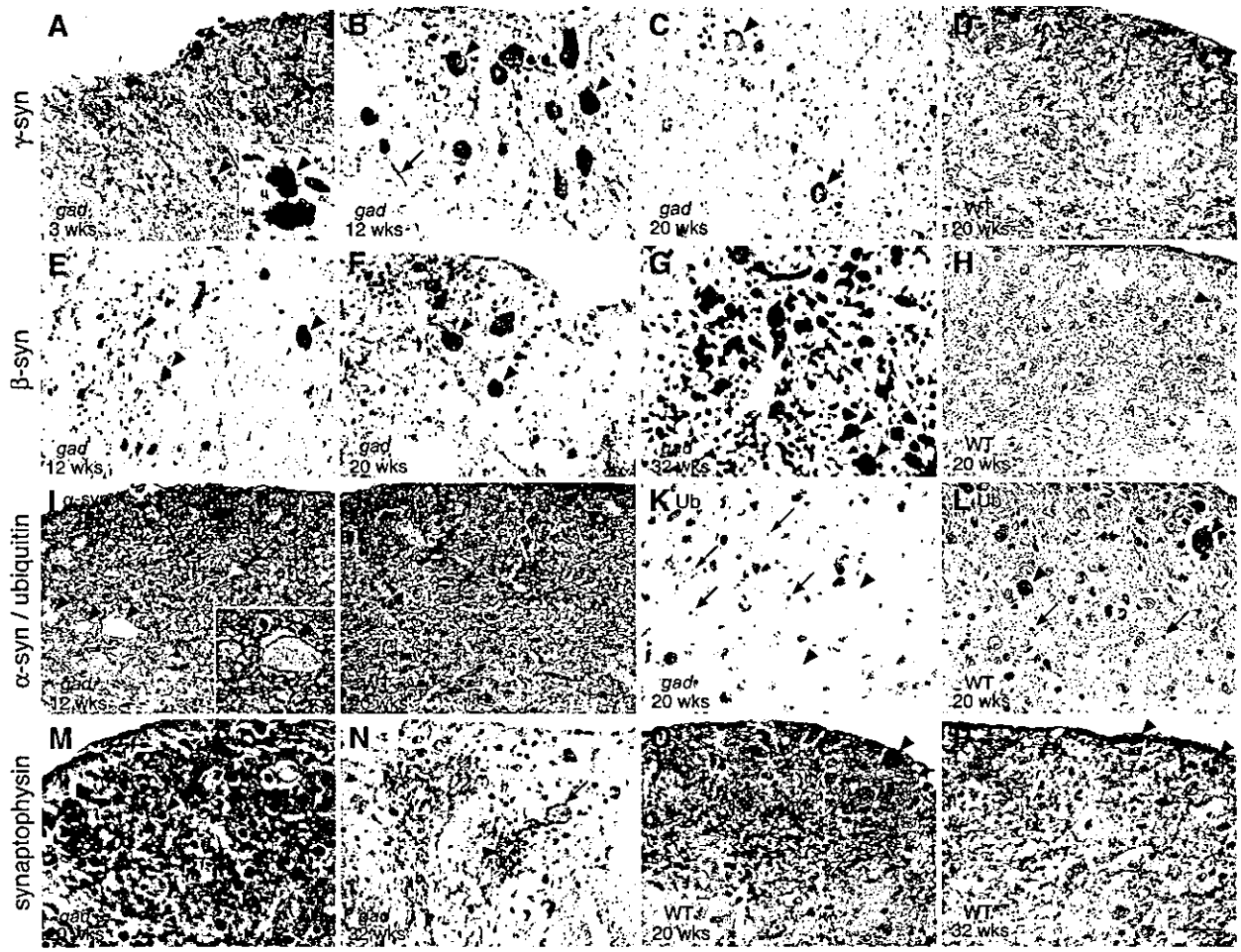

Fig. 4. Synucleins, synaptophysin and ubiquitin immunoreactivities of the gracile nucleus. Almost all spheroids showed strong immunostaining for (A–C) γ-syn and (E–G) β-syn in the gracile nucleus of gad mice from 3 to 32 weeks of age (A, 3 weeks; B and E, 12 weeks; C and F, 20 weeks; G, 32 weeks). Numerous γ-syn-positive spheroids (B, arrowheads) and occasional neurites (B, arrow) are demonstrated. Spheroids from wild-type mice at 20 weeks were also immunopositive for (D) γ-syn (arrowheads) and (H) β-syn (arrowhead). (I) Very little α-syn immunoreactivity was observed in *gad* mouse spheroids (12 weeks, arrowheads). (J) Also, as a positive control, there are any synaptic regions that could be indicated as being positive of α-syn in wild-type mouse (arrows) as well as in gad mouse (I, arrows), but α-syn was not detected in wild-type mouse spheroids (20 weeks, arrowheads). (K) Ubiquitin immunoreactivity in the *gad* mouse gracile nucleus (20 weeks) appeared in dots (arrows) but was not apparent in spheroids (arrowheads). (L) Ubiquitin-positive immunoreactivity was seen in both spheroids (arrowheads) and dots (arrows) in wild-type mice (20 weeks). For synaptophysin, except for the similar immunostaining pattern of synapses, the limited number of spheroids that were immunopositive exhibited diffuse or spotty staining (arrowheads) that was seen only in the center of spheroids at 20 weeks in both (M) *gad* and (0) wild-type mice. Indeed, *gad* mice had more synaptophysin immunoreactivity than did wild-type mice. (N) At 32 weeks, *gad* mice displayed a punctate distribution pattern of synaptophysin along synapses (arrowhead) or surrounding cell bodies, with a few densely stained spheroids (arrow). (P) In contrast, wild-type mice displayed an in situ expression pattern that was enriched in the spheroids at 32 weeks of age (arrowheads). Bar = 50 μm.

possible temporal relationships between spheroid formation and α-, β- and γ-synucleins in the *gad* mouse brain has not yet been proven. Because the *gad* mouse constitutes a neurodegenerative model for the study of spheroid proliferation in axonal termini, we therefore examined spheroid pathology using antibodies directed against α-, β- and γ-syn. Given that dystrophic swollen axons—the primary *gad* lesion observed in the gracile nucleus—result from spheroid proliferation, we quantitated spheroid formation and immunoreactivity in the medulla and upper cervical spinal cord regions over the lifetime of *gad* mice (Fig. 2F and Table 1).

We initially found that γ-syn-positive spheroids were more conspicuous than HE-stained spheroids during the early stage of age, suggesting that γ-syn is more sensitive and specific than HE for detecting spheroid formation in *gad* mice. β-syn was first detected in spheroids 8 weeks later than γ-syn. This result raises the possibility that the mechanism by which β-syn accumulates in spheroids differs from that of γ-syn and that γ-syn may play a more important role in the pathogenesis of the *gad* mutation. A recent study suggested that synucleins may help to regulate proteasome function by modulating 20S proteasome activity in the case

Table 1
Chronological change in the degree of immunoreactivity for spheroids stained for α-, β- and γ-synuclein and ubiquitin in the medulla and upper cervical cord of *gad* mice

	gad 3 weeks	*gad* 12 weeks	*gad* 20 weeks	*gad* 32 weeks	Wild-type 20 weeks	Wild-type 32 weeks
α-syn	−[a]	±	±	±	−	−
β-syn	−	+	++	+++	+	+
γ-syn	++	++	+++	+	+	+
ub-s[b]	−	−	−	−	+	+
ub-d[c]	−	++	+++	+	+	+

[a] Immunoreactivity: +++, strong; ++, moderate; + to ±, weaker to weak; −, not detectable.
[b] Ubiquitin immunoreactivity in the spheroids.
[c] Ubiquitin immunoreactivity in the dot-like structures.

of γ-syn and by affecting the 26S proteasome in the case of β-syn [34]. Thus, the fact that each of these two synucleins exhibits a distinct time course of spheroid accumulation may reflect differences in their metabolic regulation. Furthermore, γ-syn has a very different pattern of localization in neurons as compared with α-syn and β-syn [27].

Antibodies to ubiquitin recognize most spheroids, although it is unclear whether this recognition reflects sequestered free ubiquitin or ubiquitinated proteins [25,39]. Furthermore, the ubiquitinated substrates in spheroids have not been identified. We show here in *gad* mice that ubiquitin is absent from spheroids but is present in dot-like structures, which is consistent with a previous study [40]. Recently, we demonstrated that the loss of functional UCH-L1 leads to a decrease in free ubiquitin in *gad* mice [24]. In contrast, overexpression of UCH-L1 causes an increase in ubiquitin in both cultured cells and mice [24]. Therefore, we suggest that UCH-L1 ensures ubiquitin stability via prolonging the ubiquitin half-life within neurons as an important carrier protein, and loss of functional UCH-L1 may thus lead to inadequate ubiquitination via a decrease in free ubiquitin. Thus, the reduction in ubiquitin might be responsible for the absence of ubiquitin in *gad* mouse spheroids. Ubiquitin is, however, often detected in spheroid bodies during neurodegenerative diseases [2,41]. In addition, an increase in ubiquitin expression was reported in spheroid bodies in the brains of aged monkeys [31]. Despite the presence of ubiquitin in spheroid bodies in these systems, our data indicate that ubiquitination may not be required for the formation of spheroid bodies.

We found that spheroids were positive for both β- and γ-syn but were slight for α-syn in *gad* mice. Lewy bodies in PD and DLB brains are positive for both α-syn [36] and UCH-L1 [20], whereas we did not detect Lewy bodies or Lewy neurites in *gad* mouse brain. These observations suggest that the molecular mechanism of β- and γ-syn accumulation in *gad* spheroids is different from that in Lewy bodies. β-syn inhibits fibril accumulation of α-syn [11]. Thus, early accumulation of β-syn in the spheroids of *gad* mice may inhibit the accumulation of α-syn in spheroids or axon terminals. It remains unclear whether γ-syn has a similar effect on the accumulation of α-syn. Alternatively, fibril formation of α-syn might be affected by the existence of UCH-L1, and lack of UCH-L1 in the *gad* mouse might result in the suppression of α-syn aggregation in vivo. UCH-L1 was reported to have ubiquitin ligase activity that increased the amount of polyubiquitinated α-syn via K63-linked ubiquitination [19]. Other recent studies have shown that UCH-L1 can deubiquitinate polyubiquitinated α-syn with K48-linked ubiquitination [13,30]. Thus, a close relationship between UCH-L1 and α-syn has been implicated. Aggregates of β-syn and γ-syn have been found in dystrophic neurites associated with PD and other neurodegenerative diseases [7]. Neither protein, however, is detected in Lewy bodies in PD and DLB. Consequently, β-syn and γ-syn pathology may be more specific to spheroid disorders.

Pathological accumulations of β-syn and γ-syn were previously reported in neurological diseases [7]. β-syn is a presynaptic protein and *gad* degeneration starts at the presynapse of the gracile nuclei. Local accumulated β-syn may interfere with other presynaptic proteins in the degenerating terminals. We observed that a presynaptic protein, synaptophysin, was weakly detected in spheroids but strongly expressed in healthy synapses in *gad* mice. This result may support the idea of the effect of locally accumulated β-syn.

Overexpression of γ-syn may influence neurofilament network integrity [4]. Distinct from wild-type mice, in *gad* mice γ-syn immunoreactivity in the spheroids appeared in the gracile nucleus from an early stage, which might contribute to the dysfunction of the nervous system, possibly by interrupting axonal transport. Ubiquitin is known to be transported over long distances via slow axonal transport to synapses [3]. Ubiquitin reduction and the consequent inadequate ubiquitination of proteins may trigger accumulation of proteins that should undergo ubiquitin-dependent degradation. An age-dependent increase in γ- and β-syn-positive spheroids in *gad* mice resembles the accumulation of amyloid-β in spheroids of these mice [12]. Amyloid precursor protein has been shown to be transported by a fast axonal flow [16]. The abnormal accumulation of various proteins at terminals might affect axonal transport from the ganglia, leading to the dying-back type of degeneration of axons with formation of spheroid bodies. The mechanisms involved, however, will require more detailed studies of UCH-L1 and synucleins.

Acknowledgements

We thank Miss S. Kikuchi for assistance in preparation of the sections and Ms. M. Shikama for the care and breeding of animals. This work was supported in part by Grants-in-Aid for Scientific Research from the Ministry of Health, Labour and Welfare of Japan; Grants-in-Aid for Scientific Research from the Ministry of Education, Culture, Sports,

Science and Technology of Japan; a grant from the Organization for Pharmaceutical Safety and Research; and a grant from the Japan Science and Technology Agency.

References

[1] J. Aicardi, P. Castelein, Infantile neuroaxonal dystrophy, Brain 102 (1979) 727–748.

[2] N. Arai, Grumose or foamy spheroid bodies involving astrocytes in the human brain, Neuropathol. Appl. Neurobiol. 21 (1995) 238–245.

[3] A. Bizzi, B. Schaetzle, A. Patton, P. Gambetti, L. Autilio-Gambetti, Axonal transport of two major components of the ubiquitin system: free ubiquitin and ubiquitin carboxyl-terminal hydrolase PGP 9.5, Brain Res. 548 (1991) 292–299.

[4] V.L. Buchman, J. Adu, L.G. Pinon, N.N. Ninkina, A.M. Davies, Persyn, a member of the synuclein family, influences neurofilament network integrity, Nat. Neurosci. 1 (1998) 101–103.

[5] V.L. Buchman, H.J. Hunter, L.G. Pinon, J. Thompson, E.M. Privalova, N.N. Ninkina, A.M. Davies, Persyn, a member of the synuclein family, has a distinct pattern of expression in the developing nervous system, J. Neurosci. 18 (1998) 9335–9341.

[6] M. Farrer, J. Kachergus, L. Forno, S. Lincoln, D.S. Wang, M. Hulihan, D. Maraganore, K. Gwinn-Hardy, Z. Wszolek, D. Dickson, J.W. Langston, Comparison of kindreds with parkinsonism and alpha-synuclein genomic multiplications, Ann. Neurol. 55 (2004) 174–179.

[7] J.E. Galvin, K. Uryu, V.M. Lee, J.Q. Trojanowski, Axon pathology in Parkinson's disease and Lewy body dementia hippocampus contains alpha-, beta-, and gamma-synuclein, Proc. Natl. Acad. Sci. U. S. A. 96 (1999) 13450–13455.

[8] J.E. Galvin, B. Giasson, H.I. Hurtig, V.M. Lee, J.Q. Trojanowski, Neurodegeneration with brain iron accumulation, type 1 is characterized by alpha-, beta-, and gamma-synuclein neuropathology, Am. J. Pathol. 157 (2000) 361–368.

[9] M. Goedert, M.G. Spillantini, Dewy body diseases and multiple system atrophy as alpha-synucleinopathies, Mol. Psychiatry 3 (1998) 462–465.

[10] W. Halliday, The nosology of Hallervorden-spatz disease, J. Neurol. Sci. 134 (1995) 84–91 (Suppl.).

[11] M. Hashimoto, E. Rockenstein, M. Mante, M. Mallory, E. Masliah, beta-synuclein inhibits alpha-synuclein aggregation: a possible role as an anti-parkinsonian factor, Neuron 32 (2001) 213–223.

[12] N. Ichihara, J. Wu, D.H. Chui, K. Yamazaki, T. Wakabayashi, T. Kikuchi, Axonal degeneration promotes abnormal accumulation of amyloid beta-protein in ascending gracile tract of gracile axonal dystrophy (GAD) mouse, Brain Res. 695 (1995) 173–178.

[13] Y. Imai, M. Soda, R. Takahashi, Parkin suppresses unfolded protein stress-induced cell death through its E3 ubiquitin-protein ligase activity, J. Biol. Chem. 275 (2000) 35661–35664.

[14] T. Kikuchi, M. Mukoyama, K. Yamazaki, H. Moriya, Axonal degeneration of ascending sensory neurons in gracile axonal dystrophy mutant mouse, Acta Neuropathol. (Berl.) 80 (1990) 145–151.

[15] Y. Kon, D. Endoh, T. Iwanaga, Expression of protein gene product 9.5, a neuronal ubiquitin C-terminal hydrolase, and its developing change in sertoli cells of mouse testis, Mol. Reprod. Dev. 54 (1999) 333–341.

[16] E.H. Koo, S.S. Sisodia, D.-R. Archer, L.J. Martin, A. Weidemarm, K. Beyreuther, P. Fischer, C.L. Masters, D.L. Price, Precursor of amyloid protein in Alzheimer disease undergoes fast anterograde axonal transport, Proc. Natl. Acad. Sci. U. S. A. 87 (1990) 1561–1565.

[17] R. Kruger, W. Kuhn, T. Muller, D. Woitalla, M. Graeber, S. Kosel, H. Przuntek, J.T. Epplen, L. Schols, O. Riess, Ala30Pro mutation in the gene encoding alpha-synuclein in Parkinson's disease, Nat. Genet. 18 (1998) 106–108.

[18] C. Lavedan, E. Leroy, A. Dehejia, S. Buchholtz, A. Dutra, R.L. Nussbaum, M.H. Polymeropoulos, Identification, localization and characterization of the human gamma-synuclein gene, Hum. Genet. 103 (1998) 106–112.

[19] Y. Liu, L. Fallon, H.A. Lashuel, Z. Liu, P.T. Lansbury Jr., The UCH-L1 gene encodes two opposing enzymatic activities that affect alpha-synuclein degradation and Parkinson's disease susceptibility, Cell 111 (2002) 209–218.

[20] J. Lowe, H. McDermott, M. Landon, R.J. Mayer, K.D. Wilkinson, Ubiquitin carboxyl-terminal hydrolase (PGP 9.5) is selectively present in ubiquitinated inclusion bodies characteristic of human neurodegenerative diseases, J. Pathol. 161 (1990) 153–160.

[21] H. Miura, K. Oda, C. Endo, K. Yamazaki, H. Shibasaki, T. Kikuchi, Progressive degeneration of motor nerve terminals in GAD mutant mouse with hereditary sensory axonopathy, Neuropathol. Appl. Neurobiol. 19 (1993) 41–51.

[22] M. Mukoyama, K. Yamazaki, T. Kikuchi, T. Tomita, Neuropathology of gracile axonal dystrophy (GAD) mouse. An animal model of central distal axonopathy in primary sensory neurons, Acta Neuropathol. (Berl) 79 (1989) 294–299.

[23] K. Nishikawa, H. Li, R. Kawamura, H. Osaka, Y.L. Wang, Y. Hara, T. Hirokawa, Y. Manago, T. Amano, M. Noda, S. Aoki, K. Wada, Alterations of structure and hydrolase activity of parkinsonism-associated human ubiquitin carboxyl-terminal hydrolase L1 variants, Biochem. Biophys. Res. Commun. 304 (2003) 176–183.

[24] H. Osaka, Y.L. Wang, K. Takada, S. Takizawa, R. Setsuie, H. Li, Y. Sato, K. Nishikawa, Y.J. Sun, M. Sakurai, T. Harada, Y. Hara, I. Kimura, S. Chiba, K. Namikawa, H. Kiyama, M. Noda, S. Aoki, K. Wada, Ubiquitin carboxy-terminal hydrolase L1 binds to and stabilizes monoubiquitin in neuron, Hum. Mel. Genet. 12 (2003) 1945–1958.

[25] Y. Oya, H. Nakayasu, N. Fujita, K. Suzuki, Pathological study of mice with total deficiency of sphingolipid activator proteins (SAP knockout mice), Acta Neuropathol. (Berl.) 96 (1998) 29–40.

[26] M.H. Polymeropoulos, C. Lavedan, E. Leroy, S.E. Ide, A. Dehejia, A. Dutra, B. Pike, H. Root, J. Rubenstein, R. Boyer, E.S. Stenroos, S. Chandrasekharappa, A. Athanassiadou, T. Papapetropoulos, W.G. Johnson, A.M. Lazzarini, R.C. Duvoisin, G. Di Iorio, L.I. Golbe, R.L. Nussbaum, Mutation in the alpha-synuclein gene identified in families with Parkinson's disease, Science 276 (1997) 2045–2047.

[27] M.C. Quilty, W.P. Gai, D.L. Pountney, A.K. West, J.C. Vickers, Localization of alpha-, beta-, and gamma-synuclein during neuronal development and alterations associated with the neuronal response to axonal trauma, Exp. Neurol. 182 (2003) 195–207.

[28] K. Saigoh, Y.L. Wang, J.G. Suh, T. Yamanishi, Y. Sakai, H. Kiyosawa, T. Harada, N. Ichihara, S. Wakana, T. Kikuchi, K. Wada, Intragenic deletion in the gene encoding ubiquitin carboxy-terminal hydrolase in gad mice, Nat. Genet. 23 (1999) 47–51.

[29] K. Saito, T. Yokoyama, M. Okaniwa, S. Kamoshita, Neuropathology of chronic vitamin E deficiency in fatal familial intrahepatic cholestasis, Acta Neuropathol. (Berl) 58 (1982) 187–192.

[30] D.M. Sampathu, B.I. Giasson, A.C. Pawlyk, J.Q. Trojanowski, V.M. Lee, Ubiquitination of alpha-synuclein is not required for formation of pathological inclusions in alpha-synucleinopathies, Am. J. Pathol. 163 (2003) 91–100.

[31] C. Schultz, E.J. Dick, A.B. Cox, G.B. Hubbard, E. Braak, H. Braak, Expression of stress proteins alpha B-crystallin, ubiquitin, and hsp27 in pallido-nigral spheroids of aged rhesus monkeys, Neurobiol. Aging 22 (2001) 677–682.

[32] R. Sidman, J.B. Angevine, E.T. Pierce, Atlas of the Mouse Brain and Spinal Cord, Harvard Univ. Press, Cambridge, 1971.

[33] A.B. Singleton, M. Farrer, J. Johnson, A. Singleton, S. Hague, J. Kachergus, M. Hulihan, T. Peuralinna, A. Dutra, R. Nussbaum, S. Lincoln, A. Crawley, M. Hanson, D. Maraganore, C. Adler, M.R. Cookson, M. Muenter, M. Baptista, D. Miller, J. Blancato, J. Hardy, K. Gwinn-Hardy, Alpha-synuclein locus triplication causes Parkinson's disease, Science 302 (2003) 841.

[34] H.M. Synder, K. Mensah, I. Surgucheva, B. Festoff, A. Matouschek, A. Surguchov, B. Wolozin, Effect of alpha, beta and gamma synuclein